Investigating Structural and Functional Pathology in Cocaine use Disorder

Thesis submitted in partial fulfillment
of the requirements for the degree of

Master of Science
in
Electronics and Communication by Research

by

Duvvada Sai Siddharth
2018122006
sai.siddharth@research.iiit.ac.in

International Institute of Information Technology
Hyderabad - 500 032, INDIA
November 2023

International Institute of Information Technology
Hyderabad, India

CERTIFICATE

It is certified that the work contained in this thesis, titled 'Investigating Structural and Functional pathology in Cocaine use Disorder' by Duvvada Sai Siddharth, has been carried out under my supervision and is not submitted elsewhere for a degree.

Date

Adviser: Prof. Vinoo Alluri

To the **extraordinary** individuals who have stood by my side during the toughest of times.

Acknowledgments

I want to express my sincere gratitude to Prof.Vinoo Alluri for her patience and encouragement. Your willingness to listen and provide valuable insights, even during your busy schedule, has significantly impacted my academic and personal growth. I sincerely appreciate your responsiveness whenever I seek your advice. Your ability to provide constructive feedback encouraged me to think critically. Your mentorship has been instrumental in helping me overcome both personal and academic challenges.

It is my blessing to have such a supportive and understanding family. I cannot be thankful enough to them. I bid farewell to a cherished member of my family, Myny. May your spirit run free and your tail wag in eternal happiness.

I am thankful to Nishanth and Shrish for making my 5th year exciting. I also like to thank Rajsekhar, Abhinav, Deeksha, Samanvaya, Anurag, Shivani and Krishna for the friendships we forged, the late-night chit-chat, the laughter and the memories we shared will forever hold a special place in my heart.

Abstract

Cocaine use disorder (CUD) is a compulsive urge to seek and consume cocaine despite the inimical consequences. MRI studies from different modalities have shown that CUD patients exhibit structural and/or functional connectivity pathology among several brain regions. Nevertheless, both connectivities are commonly studied and analyzed separately, which may potentially obscure its relationship between them, and with the clinical pathology. Here, we compare and contrast structural and functional brain networks in CUD patients and healthy controls (HC). The existing body of research has predominantly concentrated on studying substance abuse within the Caucasian population. Gaining a comprehensive understanding of the distinctive challenges and cultural environments in which substance abuse disorders emerge among various populations is essential. For this study, we recruited 105 individuals of Mexican descent and carefully examined the T1-weighted, diffusion weighted imaging, resting-state fc-fMRI sequences and clinical metrics of these participants.

Based on the previous work [53], we identified regions of interest (ROIs) that are known to have altered structural connectivity in CUD patients and examined their pairwise functional connectivity. The results demonstrated that CUD exhibited stronger connection between the right Posterior Cingulate and right Postcentral than HC which could suggest an increase in interoception potentially associated with compulsion behavior.

We computed a battery of graph-based measures from multi-shell diffusion-weighted imaging (tc-dMRI) and resting state fc-fMRI to quantify local and global connectivity. We investigated the differences in functional and structural modalities between the two groups independently. Unimodal analysis showed an increase in the participation coefficient in Striatum among CUD compared to HC in the fc-fMRI modality which has been previously linked to the compulsive drug-seeking behavior observed in CUD.

Multimodal fusion is a data driven approach that involves fusion of different brain modalities to gain a more comprehensive understanding of the brain's structure and function. Multimodal fusion has played an important role in investigating joint functional and structural changes in neurological disorders like Alzheimer's disease, schizophrenia, and epilepsy. This is the first

study that uses multimodal fusion of graph theoretical measures to investigate topological alterations in CUD patients.

We specifically used multimodal canonical component analysis plus joint independent component analysis (mCCA+jICA) to evaluate group differences and their association with clinical scores. When performing multimodal fusion analysis, we observed a higher betweenness centrality and lower participation coefficient in CUD patients indicating reorganization of functional networks. In addition to altered straiatal connectivity revealed by the unimodal approach, multimodal fusion revealed latent information about brain regions involved in impairment due to cocaine abuse.

Overall, results revealed by our study not only concord with previous research in the field but also uncovered findings which could help in understanding the pathology of CUD and develop better pre-treatment/post-treatment intervention design.

Contents

List of Figures

List of Tables

Chapter 1

Introduction

1.1 Motivation

Substance abuse disorders (SUDs) are a major public health concern, affecting millions of people worldwide. SUDs are characterized by a persistent pattern of use of a substance, despite negative consequences. One of the key challenges in treating SUDs is understanding how substance use affects brain function. Recent advances in neuroimaging techniques have made it possible to investigate the neural mechanisms underlying SUDs and to identify potential targets for treatment. One of the key features of SUDs is the development of tolerance and dependence. Tolerance refers to the need for increasing amounts of a substance to achieve the same effect, while dependence refers to the development of withdrawal symptoms when the substance is discontinued. By identifying the neural mechanisms underlying SUDs, researchers can identify potential targets for treatment and develop interventions to improve brain function in individuals with SUDs.

Cocaine use disorder (CUD) is a substance use disorder (SUD), described as a compulsive urge to seek and consume cocaine despite the inimical consequences. CUD causes a gradual decline in the patient's cognitive and behavioral health [68], along with greater health and socioeconomic issues. Chronic cocaine use is suggested to cause a lack of control over consumption, leading to impulsive behaviors, medical complications, pleasure-reinforced compulsions, psychosocial problems and an intense feeling of wanting during drug abstinence (craving) [12] [43].

Understanding the unique challenges and cultural contexts in which substance abuse disorders manifest among different populations is crucial for effective prevention, intervention, and treatment strategies. However, most of the research literature has primarily focused on the Caucasian population. In this study we worked on a dataset that comes from a cross-sectional case-control study carried out in Mexico city.

Brain modalities are frequently examined and analysed separately but by combining different modalities, researchers can identify brain abnormalities associated with disorders such as Alzheimer's disease, schizophrenia, and epilepsy. This approach is called multimodal fusion and it has been instrumental in studying neurological disorders. We employed multimodal fusion to identify specific regions and circuits in the brain impacted by substance use disorders for the identification of biomarkers and to build medical interventions.

Research on the function and structure of the human brain in SUDs has been motivated by several factors. Firstly, addiction is a chronic disease that often leads to relapse, and there is a pressing need for more effective treatments. Secondly, advances in neuroscience techniques have enabled researchers to investigate the brain at the molecular, cellular, and systems level, providing unprecedented insights into the underlying mechanisms of addiction. Finally, the societal and economic impact of addiction is enormous, with costs related to healthcare, criminal justice, and lost productivity estimated to be in the billions of dollars.

1.2 Research Gap

MRI studies from different modalities have shown that CUD patients exhibit structural and/or functional connectivity pathology among a wide variety of regions such as frontal (orbitofrontal, prefrontal, cingulate cortex and insula), parietal (precuneus), temporal gyri (superior and middle temporal gyrus) and subcortical regions (ventral tegmental area, hippocampus, striatum and amygdala), including white matter tracts that connect these regions [27][21]. A recent meta-analysis showed that CUD patients display lower volume in the orbitofrontal cortex, temporal pole, anterior insula, anterior thalamic radiation, cingulum, inferior occipito-frontal fascicle and acoustic radiation [47]. Some studies also highlight brain network pathology using graph theory in CUD with non-consistent significant results [10] [75] [69]. Nevertheless, structural and functional pathology is commonly studied and analyzed separately, which may potentially obscure the relationship between them and with clinical pathology.

Fusing modalities provides a means to reveal complicated hidden relationships between modalities and weak latent effects in high-dimensional data by taking advantage of the presence of cross-information in cross-individual variance [59] [7]. For example, structural MRI can reveal changes in brain volume and cortical thickness, while functional MRI can be used to study brain activity during different tasks or in resting state. Diffusion-weighted imaging can provide information about the integrity of white matter tracts, which are critical for communication between different brain regions. By fusing these different types of MRI data, researchers can identify specific regions and circuits in the brain that are affected by substance use disorders, as well as changes in connectivity between these regions. This information can provide insights

into the underlying neural mechanisms of addiction and inform the development of targeted interventions.

Furthermore, multimodal fusion has the added benefit of increased robustness to modality-specific noise [7] and has been used in different brain pathologies like schizophrenia, bipolar and obsessive-compulsive disorders [60] [44] [25]. A recent study by Meade et al. [37] explored multimodal fusion techniques, namely multimodal canonical component analysis (mCCA) in conjunction with joint independent component analysis (jICA) on a CUD group using whole-brain voxel-wise maps and their relation with the delay discounting process.

The relevance of multimodal fusion techniques can be leveraged to develop models that exploit the data and minimize incorrect conclusions in psychiatric disorders [59] [7].

1.3 Research Objectives

Through this thesis, we aim to

- Understand intramodal relationships by analyzing tc-dMRI and resting state fc-fMRI independently.
  - Assess the reliability of the results revealed by Rasgado-Toledo et al [53] by performing seed based functional connectivity analysis
  - Investigate topological alterations in the structure and function of the brain using graph theory
- Find network-based connectivity differences using graph theory, between patients with cocaine use disorder (CUD) and matched healthy controls (HC) using tc-dMRI and resting-state fc-fMRI to reveal hidden relationships between the modalities using multimodal fusion.

1.4 Research Overview

1.5 Contributions

The central problem of this thesis is "Structural and functional pathology in cocaine use disorder with polysubstance use". We used resting-statefc-fMRI and tc-dMRI data and systematically analyzed it to identify the group differences between CUD patients and HC. The major contributions of this thesis are as follows:

- Unimodal analysis was performed to investigate brain network differences from the perspective of each modality (resting-state fc-fMRI and tc-dMRI). Global and local graph

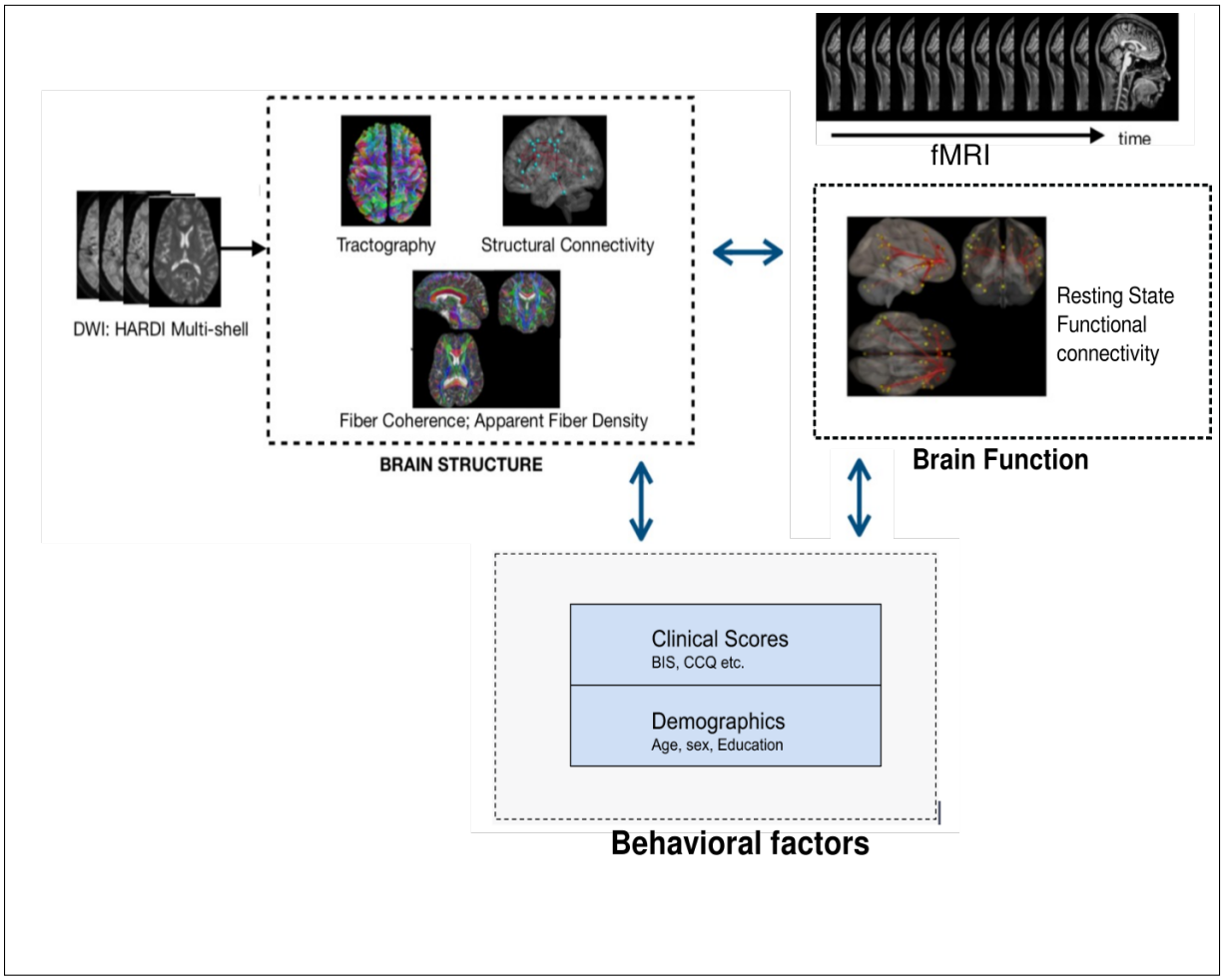

Figure 1.1 Overview of the modalities that are fused to obtain a holistic view of brain dynamics arising from structure and function, modulated by behavioural factors.

measures were analyzed to understand the functional and structural connectivity of the different brain regions. The global and local graph measures within each modality were tested for differences between CUD and HC using the Mann-Whitney-Wilcoxon test for independent two-samples. Spearman correlation between the graph measures and their corresponding clinical scores within each modality was performed. The results showed that the left Caudate exhibited a significant decrease in PC among CUD compared to HC in the resting-state fc-fMRI modality.

- We examined the macroscopic network-based differences using graph theory, between patients with cocaine use disorder (CUD) and matched healthy controls (HC) by combining resting-state fc-fMRI and tc-dMRI imaging modalities. While multimodal fusion has been carried out in other studies, to our knowledge, this is the first multimodal-fusion study that uses graph theory to explore topological alterations in CUD patients. Multimodal fusion analysis was performed using Multimodal canonical component analysis plus joint independent component analysis (mCCA+jICA). The results revealed a higher centrality of the interrelationship and a lower participation coefficient in patients with CUD. In contrast to the unimodal approach, the multimodal fusion method was able to reveal latent information about brain regions involved in impairment due to cocaine abuse. These results could help in understanding the pathology of CUD in order to develop better pre-treatment/post-treatment intervention designs.

1.6 Thesis Overview

Magnetic Resonance Imaging (MRI) studies can provide valuable insights into the neurological effects of cocaine use disorders (CUD. In this thesis, we discuss the findings of unimodal and multimodal analysis of CUD patients and healthy controls (HC).

- Chapter 2 provides an overview of the existing CUD literature and delves into relevant MRI studies. It also provides an overview of techniques such as multimodal fusion analysis, which have been used to leverage multimodal information to improve the accuracy and specificity of MRI-based neuro-ailment diagnosis, with a focus on CUD research.

- In Chapter 3, the image acquisition and pre-processing steps for the data used in this thesis are elaborated. The pre-processing method is vital for MRI studies as there are numerous confounding factors that can affect the observations. The fMRIprep pipeline (21) is explained, and demographic information for CUD and HC subjects is presented. Furthermore, we have provided an overview of the various tools and techniques used in the subsequent chapters. These include the various graph theoretical measures (global and local measures), along with their significance. We have also given an overview of the algorithms used to calculate these graph measures.

- In Chapter 4, the unimodal analysis of CUD and HC groups is discussed. It is based on the analysis of static connectivity. Both diffusion-based structural connectivity (tc-dMRI) and resting state functional connectivity (rs-fMRI) are abstracted as graphs, where each connection denotes the association between the two regions. We used several graph theoretical measures like Assortativity (r), Network efficiency (Eglobal), Modularity (M), Smallworld index (σ), and Hierarchy (β). Local measures include Betweenness Centrality (BC), Degree Centrality (DC), Participation Coefficient (PC), Nodal Local Efficiency (NLE) and Nodal clustering Coefficient (NCC) to identify differences between CUD and HC.
- In Chapter 5, we demonstrate a multimodal fusion of graph theoretical measures computed on tc-dMRI and rs-fMRI modalities, an alternative way of quantifying network changes in CUD and HC using resting state data. We used joint independent component analysis (jICA) and Multimodal canonical component analysis plus joint independent component analysis (mCCA+jICA) to compare between techniques. We then used statistical tests to evaluate group differences and their association with clinical alterations. Using a multimodal approach, we understand the structural and functional pathology in CUD and its relationship with clinical manifestations
- Chapter 7 ends by addressing the limitations of this study as well as potential future applications.

Chapter 2

Background

In the last decade, neuroimaging has grown tremendously as a research method and a clinical tool in the field of substance abuse. As a result, we identified studies that looked into the effects of SUDs on structural and/or functional connectivity. This chapter provides an overview of the existing literature on such research.

2.1 NeuroImaging Techniques

The functioning of the brain is complex, and different non-invasive neuroimaging techniques (fMRI, MEG, EEG etc.) can offer a wide range of visual representations as well as a quantitative understanding of the anatomy, electrical activity, oxygen consumption and a variety of other physiological activities inside the central nervous system. Neuroimaging has evolved into a promising technique for disease diagnosis and assessing brain health, in addition to investigating how the brain function. In the subsequent sections, we discuss the two neuroimaging techniques (i.e. fMRI and DTI) used in this study.

2.1.1 Diffusion Tractography Imaging (DTI

Diffusion tractography imaging (DTI) is a non-invasive technique used to investigate the structural connectivity of the brain. By mapping the diffusion of water molecules in brain tissue, DTI can identify white matter tracts that connect different brain regions. DTI has emerged as a valuable tool for investigating the structural organization of the brain and has numerous potential applications in both clinical and research settings. One of the key advantages of DTI is its ability to investigate the structural connectivity of the brain in vivo. Structural connectivity refers to the physical connections between different regions of the brain, as opposed to functional connectivity, which refers to the degree to which neural activity in different regions of the brain is correlated. DTI can identify the white matter tracts that connect different brain regions and

provide information about the strength and directionality of these connections. DTI has been used to investigate a wide range of neurological and psychiatric disorders, including traumatic brain injury, stroke, multiple sclerosis, and schizophrenia. For example, studies using DTI have identified alterations in white matter tracts in individuals with schizophrenia, particularly in the corpus callosum, a key white matter tract that connects the two hemispheres of the brain [26]. It has also been used to investigate the structural connectivity of the brain in substance abuse disorders. Studies using DTI have identified alterations in white matter tracts in individuals with substance abuse disorders, particularly in regions involved in reward processing and executive control. For example, individuals with substance abuse disorders show decreased white matter integrity in the prefrontal cortex, a key region involved in executive control [30]

2.1.2 Functional Magnetic Resonance Imaging (fMRI)

Functional Magnetic Resonance Imaging (fMRI) is a non-invasive imaging technique used to visualize changes in the blood oxygenation level-dependent (BOLD) signal in the brain. This technique has revolutionized the field of cognitive neuroscience by allowing researchers to investigate brain function in healthy and clinical populations. The BOLD signal in fMRI is thought to reflect changes in neural activity due to the brain's metabolic demands. When neurons become active, they require more oxygen and glucose, leading to an increase in blood flow to the active region. This increase in blood flow leads to an increase in oxyhemoglobin concentration relative to deoxyhemoglobin, which can be detected by fMRI.

fMRI has been used to investigate a wide range of cognitive and perceptual processes, including attention, memory, language, emotion, and perception. One of the key strengths of fMRI is its ability to localize brain activity with high spatial resolution. Using fMRI, researchers can identify specific brain regions that are involved in different cognitive processes and investigate the interactions between these regions. It has also been used to investigate brain function in clinical populations, such as patients with neurological and psychiatric disorders. By identifying changes in brain function in these populations, researchers can gain insights into the underlying neural mechanisms of these disorders and potentially develop new treatments. One of the key advantages of fMRI is its ability to investigate functional connectivity (Fc) between different brain regions. Fc is the degree to which neural activity in different brain regions is correlated.

The two commonly used paradigms of fMRI are task-based and resting-state fMRI. Resting-state functional magnetic resonance imaging (rs-fMRI) is a technique used to study the intrinsic functional organization of the brain, independent of any specific task or stimulus. Whereas, Task-based functional magnetic resonance imaging (fMRI) is a technique used to investigate changes in brain activity in response to specific tasks or stimuli. Both approaches have proven to be valuable tools for investigating the neural mechanisms underlying different neurological and psychiatric disorders.

2.2 Literature Review of studies using Functional Connectivity

Resting-state functional Magnetic Resonance Imaging (rs-fMRI) and task-based functional Magnetic Resonance Imaging (ts-fMRI) are two commonly used techniques for investigating functional connectivity in the brain.

2.2.1 Resting-state functional Magnetic Resonance Imaging (rs-fMRI)

Several studies have used rs-fMRI to investigate the effects of cocaine use disorder on brain function. According to the earliest study by Li et al. [28] that investigated resting-state functional connectivity (rsFC) in relation to addiction, significant decreases in connectivity were observed within the primary visual and motor cortices after administering cocaine to individuals with addiction. Several studies have used rs-fMRI to investigate the effects of cocaine use disorder. For example, Hanlon et al. [21] found that cocaine users had increased connectivity between the anterior and posterior regions of the DMN, which was associated with greater craving for cocaine.

A study by Kelly et al. [24] has reported altered connectivity within the salience network SN and executive control network (ECN) in individuals with CUD. For instance, A study by Ray et al. [54] found enhanced Resting State Functional Connectivity (RSFC) within the sensory-motor cortex and the left frontal-parietal network in cocaine users compared to controls. An increased inter-network RSFC between frontal-temporal and frontal-parietal brain regions and a decreased RSFC between parietal-parietal, occipital-limbic, occipital-occipital, and occipital-parietal brain regions was also found in cocaine users. Furthermore, the study discovered that the sensory-motor cortex's intra-network connectivity strength was negatively correlated with years of cocaine use, whereas the inter-network connectivity strength between occipital-limbic brain areas was positively correlated with years of cocaine use.

When comparing cocaine[20] [62][70], prescription opioid [63] and heroin-dependent individuals with matched, non-drug using controls, changes in rsFC strength between the ventral striatum and various subcortical and cortical regions were observed. Specifically, [20] revealed that cocaine addicts had lower rsFC strength between the amygdala and an area of medial PreFrontal Cortex (PFC), including portions of ventromedial PFC and rostral Anterior Cingulate Cortex.

Similarly, a study [8] discovered increased positive connectivity between the ACC and the dlPFC in a sample of 27 active cocaine users. While the direction of this connectivity change appears counter-intuitive and contradictory to the previous results, greater rsFC in this ACC-dlPFC circuit was associated with poorer task performance during reversal learning.

2.2.2 Task-based functional Magnetic Resonance Imaging (ts-fMRI)

Task-based fMRI studies have been widely used to investigate functional connectivity in individuals with CUD. The results of the study conducted by Albein-Urios et al.[2] showed that cocaine-dependent individuals (CDI) had increased activation in the right dorsolateral prefrontal cortex and bilateral temporoparietal junction during the Maintain condition as compared to the Observe condition. In contrast, CDI showed decreased activation in the right inferior frontal gyrus, posterior cingulate cortex, insula, and fusiform gyrus during the Suppress condition as compared to the Maintain condition. Additionally, the study found that CDI had increased functional coupling between the dorsolateral prefrontal cortex and emotion-related regions during the Maintain condition and decreased functional coupling between the right inferior frontal gyrus and the amygdala during the Suppress condition and suggests that CDI have dysfunctional corticolimbic activation and connectivity during negative emotion experiences and re-appraisal.

Hanlon et al. [22] found that cocaine users had weaker connectivity in the frontal-striatal circuits compared to healthy controls. However, connectivity between different cortical regions was not affected. Moreover, the strength of the connection between the supplementary motor area and the caudate (a region in the striatum) was correlated with reaction time in finger tapping task in cocaine users, indicating that impaired connectivity may contribute to sensorimotor dysfunction in these individuals. These findings suggest that chronic cocaine use may result in fundamental deficits in information processing, which can have an impact on complex cognitive processes.

Ma et al. [33] showed that during the Hard NoGo task, the effective connectivity from right dorsolateral prefrontal cortex (DLPFC) to the left caudate became more positive, and the effective connectivity from right ventrolateral prefrontal cortex (VLPFC) to left caudate became more negative in the controls. In contrast, in Cocaine Dependent (CD) subjects, the effective connectivity from left anterior cingulate cortex (ACC) to left caudate became more negative during the Hard NoGo tasks. These results suggest that during Hard NoGo trials, the ACC rather than DLPFC or VLPFC influences caudate activity during response inhibition in CD individuals.

The study conducted by Mitchell et al. [40] found that cocaine-dependent patients had less intrinsic connectivity in cortical and sub-cortical regions compared to non-addicted individuals. The cocaine-dependent group also displayed relatively greater Stroop-related connectivity in regions implicated in motivational processes in addictions. Furthermore, non-mean-adjusted intrinsic-connectivity measures in the midbrain, thalamus, ventral striatum, substantia nigra, insula, and hippocampus negatively correlated with measures of cocaine abstinence, indicating the potential of connectivity as a treatment target.

2.3 Literature Review of studies using Structural Connectivity

Structural Magnetic Resonance Imaging (sMRI) and diffusion tensor imaging (DTI) are two commonly used techniques for investigating structural connectivity in the brain.

2.3.1 Structural Magnetic Resonance Imaging (sMRI)

Several studies have used sMRI to investigate the effects of cocaine use disorder on brain structure. A study by Ersche et al. [15] revealed that cocaine dependence was associated with decreased grey matter volume in the orbitofrontal, cingulate, insular, temporoparietal, and cerebellar cortex and with an increase in grey matter volume in the basal ganglia. Greater duration of cocaine dependence was correlated with greater grey matter volume reduction in orbitofrontal, cingulate, and insular cortex. Greater impairment of attentional control was associated with reduced volume in insular cortex and increased volume of caudate nucleus. Greater compulsivity of drug use was associated with reduced volume in orbitofrontal cortex. Cocaine-dependent individuals had abnormal structure of corticostriatal systems, and variability in the extent of anatomical changes in orbitofrontal, insular, and striatal structures was related to individual differences in duration of dependence, inattention, and compulsivity of cocaine consumption.

Similarly, Konova et al. [41] found that the group of individuals with impaired insight CUD had lower activity in the error-induced rostral anterior cingulate cortex (rACC), which was associated with more frequent cocaine use, less gray matter within the rACC, and lower levels of emotional awareness compared to controls. Similarly, Gardini et al. [17] showed that cocaine-dependent patients had lower grey matter values in the left middle occipital gyrus, right putamen, and insula, while heroin-dependent patients had lower grey matter values in the right insula. Both cocaine and heroin-dependent patients showed reduced grey matter in the right posterior insular cortex. The direct comparison between the two addiction groups showed that cocaine abusers had less grey matter in the right posterior cingulate, medio-temporal, and cerebellar regions, while heroin abusers showed less grey matter in parietal regions on both sides, including postcentral gyrus and inferior parietal lobule. Vaquero et al. [66] revealed that Cocaine- Dependent patients showed increased gray matter volume (GMV) in the caudate and the orbitofrontal cortex.

Similarly, Bachi et al. [4] investigated the contribution of childhood trauma to gray matter concentration (GMC) effects in individuals with cocaine use disorder and found that individuals with high childhood trauma had reduced GMC in the right lateral orbitofrontal cortex (OFC) compared to controls, while no significant differences were found between individuals with low childhood trauma and controls. Childhood trauma accounted for a significant amount of

variance in the GMC in the right lateral OFC, even after controlling for demographics, drug use, constraint, and depression.

2.3.2 Diffusion Tractography Imaging (DTI)

Diffusion tensor imaging (DTI) is a neuroimaging technique that measures the diffusion of water molecules in the brain. It provides information about the structural connectivity of white matter tracts in the brain and have been used to investigate the effects of chronic cocaine use on the structural connectivity of brain. For instance, in a study by Romero et al [55] showed that cocaine-dependent subjects had significantly lower fractional anisotropy values in the inferior frontal white matter at the anterior-posterior commissure plane and higher anterior cingulate white matter values than control subjects. These findings suggest that cocaine dependence may involve a disruption of orbitofrontal connectivity and that the anterior cingulate brain area might play a role in the motivation to change.

In a study by Morie et al. [42], region of interest analyses for anisotropy estimates derived from the crossing-fibre model revealed significant group differences for secondary fibers. Reduced anisotropy was observed among Prenatal cocaine exposure (PCE) adolescents compared to prenatally non-exposed youth in the right cingulum and the left superior longitudinal fasciculus (SLF).

Similarly, Lim et al. [31] showed that cocaine users had lower Fractional Anisotropy (FA) compared to controls, specifically in inferior frontal white matter and revealed that both gray and white matter inferior frontal volumes were found to be smaller in the cocaine group. The results indicated The findings revealed that the duration of use was associated with decreased gray and white matter volumes. In cocaine users, FA and grey matter volume were found to be correlated.

In a premliminary study conducted by Ma et al. [35] found that Cocaine Use Disorder (CocUD) subjects had a significantly greater change in fractional anisotropy (ΔFA) than controls in the left splenium of the corpus callosum after ten weeks. Greater ΔFA (Scan 1 FA minus scan 2 FA) in this region was associated with shorter lifetime cocaine use and a greater number of positive cocaine urine samples collected during the treatment.

2.4 Literature Review of studies using Graph Theory

In substance abuse disorders, the brain undergoes significant changes in connectivity and function, leading to addiction and other behavioral abnormalities. Graph theory analysis can provide insights into the structural and functional changes that occur in the brain during substance abuse disorders.

Schweitzer et al. [57] performed network analysis underlying visuospatial working memory (VSWM) performance and showed that the prenatal drug exposure (PDE) group had lower global efficiency than the non-exposed group and a trend-level reduction in local efficiency. The network node corresponding to the middle frontal gyrus (MFG) group by task interaction showed reduced nodal efficiency and fewer direct connections to other nodes in the network. In a study conducted by Wang et al. [69], graph theoretical analysis was used to assess Functional Connectome (FCM), and the results showed that polydrug users whose primary diagnosis was cocaine dependence (DRUG) exhibited stronger functional connectivity among the assessed 90 brain subdivisions compared to non-drug using healthy controls (CTL). However, after controlling for functional connectivity differences and network density, DRUG showed reduced communication efficiency and reduced small-worldness. This suggests a loss of normal inter-regional communications and topology features, making it difficult to inhibit drug-seeking behavior.

Pacheco et al. [45] showed that the Betweenness centrality (BC) had higher values in the (Inhaled Substance Abuse Disorder) ISAD population across regions of different subnetworks. This might be an indicator that the structural organization of the network, which underlies functional connectivity networks, is altered. The generalized greater values of the BC may be an adaptation of the network in order for it not to lose function at the cost of a less efficient information transfer.

2.5 Literature Review of studies using Multimodal Fusion

Multimodal fusion analysis of the brain involves combining data from multiple sources, such as neuroimaging, genetics, and clinical assessments, to gain a more comprehensive understanding of the substance use disorder. Meade et al. [37] used multimodal canonical component analysis plus joint independent component analysis to identify co-alterations in brain structure and function with delay discounting as the reference. The results of their study revealed that participants with CUD had higher delay discounting compared to those without CUD and identified one joint component that correlated with delay discounting across all modalities, involving regions in the thalamus, dorsal striatum, frontopolar cortex, occipital lobe, and corpus callosum. The components were negatively correlated with delay discounting, such that weaker loadings were associated with higher discounting. The component loadings were lower in persons with CUD, meaning the component was expressed less strongly. The findings reveal structural and functional co-alterations linked to delay discounting, particularly in brain regions involved in reward salience, executive control, and visual attention and connecting white matter tracts. These multimodal networks were weaker in persons with CUD, indicating less cognitive control that may contribute to impulsive behaviors.

Chapter 3

Dataset and Methods

3.1 Participants

The sample consisted of 63 (8 females) cocaine use disorder patients (CUD) and 42 (9 females) healthy controls (HC), part of the SUDMEX CONN database [3]. The database comprised a set of CUD patients and controls paired by age, sex, handedness and education. We included participants who had T1-weighted, diffusion-weighted imaging and resting-state fc-fMRI sequences for this study. Due to analysis failures, three CUD patients and one HC subject were eliminated from the analysis. Demographic characteristics are shown in Table 1. According to the Declaration of Helsinki, the study was approved by the local ethics committee and carried out at the Instituto Nacional de Psiquiatría "Ramón de la Fuente Muñiz" in Mexico City, Mexico. All participants provided verbal and written informed consent. Recruitment criteria and full sample details are described in Angeles-Valdez [3].

3.2 Data Acquisition

Magnetic Resonance Imaging sequences were acquired using a Philips Ingenia 3T system (Philips Healthcare, Best, The Netherlands, and Boston, MA, USA) with a 32-channel dS Head coil. Resting-state images (rs-fMRI) were acquired using a gradient recalled (GE) echo planar imaging (EPI) sequence with the following parameters: repetition time (TR) = 2000, echo time (TE) = 30.001ms, flip angle = 75°, matrix = 80x80, FOV = 240mm2, voxel size = 3x3x3mm, number of slices=36, phase encoding direction = AP. T1-weighted (T1w) were acquired using a three-dimensional FFE SENSE sequence, TR = 7, TE = 3.5 ms, FOV = 240mm2, matrix = 240×240 mm, number of slices = 180, gap = 0, plane = sagittal, voxel = 1x1x1 mm. Subjects were instructed to keep eyes open and stare at a fixation cross presented. High Angular Resolution Diffusion Imaging (DWI-HARDI) used a SE sequence, TR = 8600 TE = 126.78 ms,

Table 3.1 Demographic characteristics of participants.

	CUD ($n = 63$)	HC(n=42)	Stats
Age	$32(18-50)$	$30(18-48)$	$t = -0.5, p = 0.6$
Education	Middle School	High School	$\chi^2 = 10, p = 0.04$
Handedness *	($n = 63$)	(n = 42)	
Right	56	35	
Left	4	4	
Ambidextrous	3	3	
Onset age of consumption	20 (12 - 41)	na	
Years consuming	10 (1 - 28)	na	
Average consumption per intake *	(n = 55)	na	
< 0.8 gm	0	na	
1.6 - 2.4 gm	7	na	
3.2 - 5.6 gm	11	na	
8 - 9 gm	26	na	
9 - 10 gm	6	na	
> 10 gm	10	na	

Notes: Median (min–max) for all except * = count. CUD = Cocaine Use Disorder, HC = Healthy controls, n = due to the absence of data, we show each sample size per variable, na = not applicable, gm = grams, Stats = statistics, t = t-value, χ^2 = chi-squared.

FOV = 224, matrix = 112x112 mm, number of slices = 50 , gap = 0, plane = axial, voxel = 2 x 2 x 2 mm, directions: 8 = b0, 36 = b-value 1,000 s/mm^2 and 92 = b-value 3,000 s/mm^2, total = 136 directions. The MRI order of acquisition was: 1) rs-MRI, 2) T1w and 3) DWI-HARDI. The total scanning time lasted around 50 minutes.

3.3 Clinical measures

Participants were evaluated using a battery of paper-based clinical questionnaires before MRI scanning. For this study, the CUD group was assessed using the Cocaine Craving Questionnaire (CCQ-General) and (CCQ-Now) to rate their craving over the previous week and at the time of MRI scanning. This questionnaire includes questions about the desire to use cocaine, the anticipation of positive outcomes and relief from withdrawal [46]. For evaluating functional im-

pairments or disabilities in psychiatric patients, the CUD group was assessed by World Health Organization Disability Assessment Schedule 2.0 (WHODAS 2.0). This instrument has been widely used in different countries for health and disabilities, finding high consistency rates [64]. Meanwhile, the CUD group was assessed by Addiction Severity Index (ASIP) for consumption status and addiction severity. This instrument is a semi-structured interview that evaluates several functional domains like medical status, employment, alcohol use, drugs use, family/social life and psychiatric status [36]. Impulsivity was also assessed using Barratt Impulsiveness Scale Version 11 (BIS-11), which is a self-report scale that assesses three categories of personality/behavioral impulsivity: cognitive (i.e. inability to focus attention), motor (i.e. act without thinking), and non-planning impulsiveness (i.e. lack of forethought) [49]. For information on other clinical measures that were recorded along with the above-mentioned, see Angeles-Valdez [3].

3.4 Overview of Methods

In Figure 3.1 illustrates an overview of the current study. A) Data from 66 (8 females) cocaine use disorder patients (CUD) and 43 (9 females) healthy controls (HC), B) Data preprocessing of Resting-state and T1-weighted MRI images were performed using fMRIprep pipeline followed by XCPengine pipeline, and FSL DWI preprocessing, C) Connectivity analysis based on Graph-based approach along with correlation with clinical measures, D) mCCA+jICA multimodal fusion based on local graph-based measures.

3.5 Clinical measures

Data preprocessing of Resting-state and T1-weighted MRI images was performed using fMRIprep pipeline [16]. Structural T1 steps included a volume correction of intensity non-uniformity, skull-stripped, brain tissue segmentation, and a spatial normalization onto MNI common brain space (MNI152NLin2009cAsym). Functional preprocessing steps included correction for intensity, slice-timing and head motion, spatial smoothing with an isotropic Gaussian kernel of 6 mm full width at half maximum (FWHM), framewise displacement threshold of 0.5, distortion estimation using a field map, skull-stripped, and a spatial normalization to MNI brain space. Resting-state time series were then processed using XCP Engine v. 1.2.1 [9] with nuisance regression using the pipeline described in Power et al. [51]. Shortly, nuisance strategy included: 1) inhomogeneities correction, 2) dummies removal (4 initial volumes), 3) realignment of all volumes to reference, 4) demeaning and removal of trends, 5) co-registration, 6) removal of global, white matter and cerebrospinal confounding signals, 7) motion scrubbing and 8) temporal filtering with a first-order Butterworth filter using a bandpass between 0.01 and 0.08 Hz. DWI-MRI preprocessing consisted in the correction of eddy current artifacts and motion

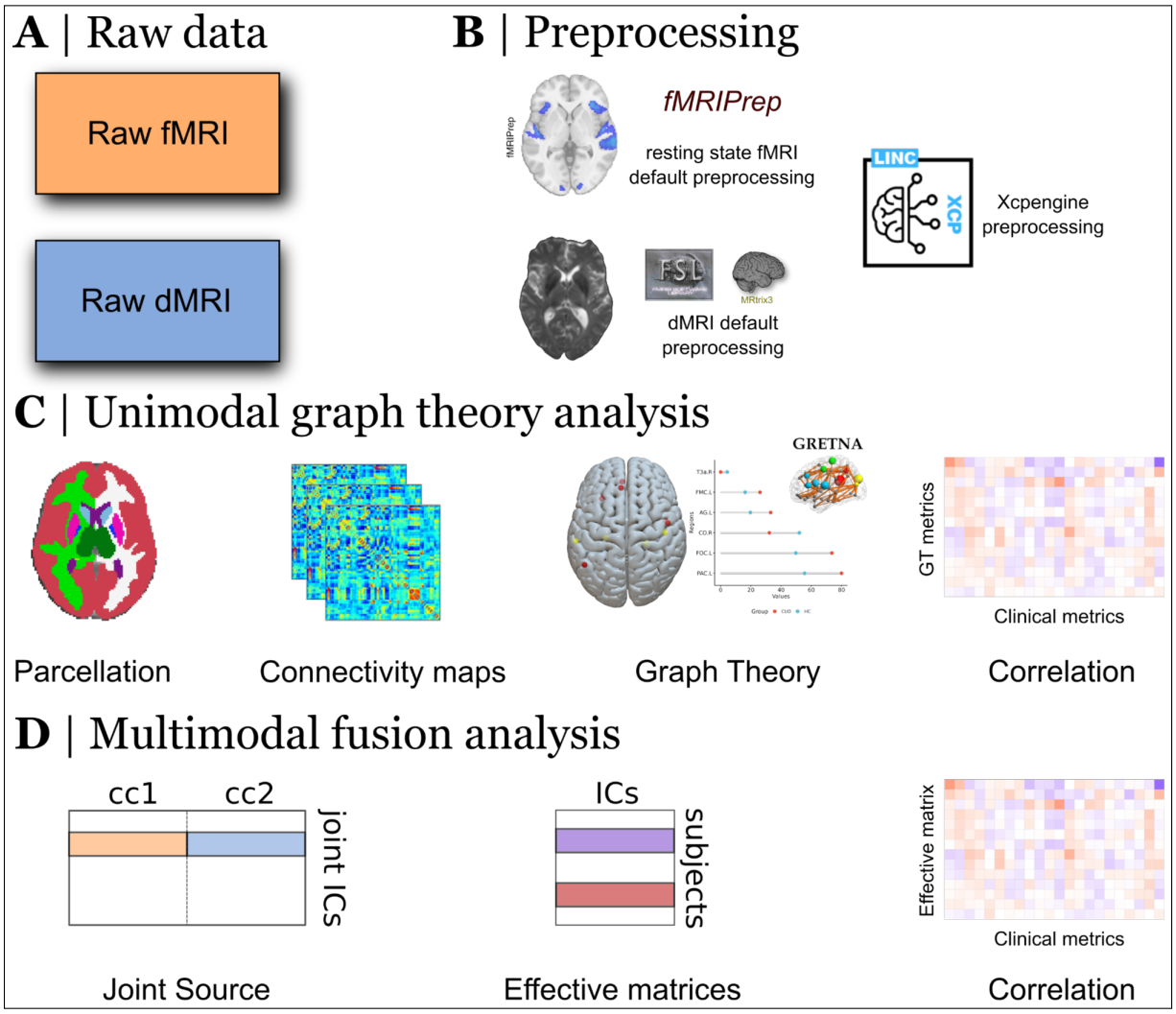

Figure 3.1 Overview of Methods

noise using eddy correct from FSL 6.0.11 (https://fsl.fmrib.ox.ac.uk). Gradients were rotated to match the affine transformation applied in the eddy step; subsequently, skull stripping was performed using the brain extraction tool from FSL. Finally, using Advanced Normalization Tools (ANTs) registration, MNI brain space was transformed into individual subject space to map all the ROI into subject space.

3.6 Global Signal Regression

fMRI data is noisy and contains unwanted signals that can affect the accuracy and reliability of the results.One of the preprocessing techniques that have gained popularity in recent years is Global Signal Regression (GSR). GSR is a technique that removes the global signal. GSR

is a preprocessing technique that removes the global signal from the fMRI data. The global signal represents the average signal across the entire brain and is considered to be a source of non-neural noise in the data. GSR involves regressing out the global signal from the fMRI data to reduce this non-neural noise.GSR removes non-neural noise from the fMRI data, such as scanner drift, physiological noise, and motion artifacts. This leads to cleaner data and reduces the impact of these unwanted signals on subsequent analysis. GSR can enhance the signal-to-noise ratio in the fMRI data. By removing non-neural noise, GSR increases the proportion of neural signal in the data, making it easier to detect subtle changes in brain activity. However, GSR can remove neural signal from the fMRI data, leading to a loss of information. The global signal contains some neural information, and removing it can affect the accuracy and reliability of subsequent analysis. GSR can also introduce negative correlations between brain regions that are not present in the original data which can lead to erroneous interpretations of functional connectivity between brain regions. We used fMRI data with GSR as well as without GSR in our analyses.

3.7 Connectivity Analyses

3.7.1 Structural Connectome

The diffusion connectivity (tc-dmri) matrices were computed using the Harvard-Oxford (HO) cortical and subcortical atlases (112 regions) and with the Desikan Killiany (DK, 86 regions) atlas through fibre-counting. For DK atlas regions, T1w structural data were processed using Freesurfer, which performed intensity bias correction, non-brain tissue discard, and tissue segmentation before performing entire brain parcellation using spherical transformation and surface-based registration with the Desikan-Killiany atlas. Connectivity maps were constructed by whole-brain streamline fiber tractography on native space using MRtrix v.3 (24). All ROIs in each atlas in sequence 1 to n-regions and the probabilistic connectome values represent the connectivity fiber counts between the source and destination ROIs. All fibers that start or end in GM-ROIs were taken into the fiber count. Normalization of all values was performed by summing the number of voxels from the source and destination ROIs. The main analysis presented here is based on the Harvard-Oxford atlas. The analysis using the Desikan Killiany atlas is presented in the Supplementary material.

3.7.2 Functional Connectome

The functional connectivity (fc-fmri) matrices were computed using the HO cortical and subcortical atlases, DK atlas. The mean time series was extracted from each region, and the functional connectivity matrix was estimated by computing pairwise Pearson correlations. Following this, the FC matrices were thresholded to generate a binary adjacency matrix that represents the

presence or absence of functional connectivity. The thresholding and binarization procedures help reduce weaker connections and result in undirected, unweighted, binary matrices where the correlations above a certain threshold are represented by 1 and 0 otherwise. Since the choice of threshold can be arbitrary, we generated several binarized adjacency matrices by varying the cut-off to include the top 5% to 50% with increments of 5%. The main analysis presented here is based on the Harvard-Oxford atlas. The analysis using the DK atlas is presented in the Supplemental Material.

3.8 Graphical Understanding of Brain

Recent advances in neuroimaging techniques have made it possible to investigate the structural and functional connectivity of the brain in great detail. One approach to exploring the connectivity of the brain is through the use of graphical models. Graphical models are mathematical tools used to represent the connectivity of complex systems. In the context of the brain, graphical models can represent structural connectivity, which refers to the physical connections between different brain regions and functional connectivity, which refers to the degree to which neural activity in different brain regions is correlated. The graph nodes represent brain regions, and the edges represent their connections. An appropriate parcellation or template must be chosen in order to build these graphs for the brain. The brain is segmented into non-overlapping, homogeneous areas through parcellations. After non-linear registration and averaging of T1 scans from numerous subjects, the standard templates are created (MNI152 is a standard template used). These regions subsequently serve as the graph's nodes or vertices. These are commonly used parcellations:

- The Automated Anatomical Labelling (AAL) 90-node parcellation.
- The Harvard-Oxford (HO) atlas with 112 areas.
- The Desikan-Killany parcellation with 86 areas.
- The Power atlas with 264 areas.

By analyzing the graphical structure of the brain, researchers can identify patterns of connectivity that may be associated with specific cognitive processes or behaviours. Graphical models have also been used to investigate alterations in brain connectivity in several neurological and psychiatric disorders.

3.9 Graph-Based Connectivity Measures

Graph theory analyses are performed on the binarized adjacency matrices using Matlab v. 2019b and the Graph Theoretical Network Analysis (GRETNA) toolbox (25). The computed

graph measures were classified into two categories based on the type of connectivity they signify global and local graph measures. These graph measures enable us to understand properties like connectivity or topology at whole-brain and region levels, respectively. Global measures comprise Assortativity (r), Network efficiency (E_{global}), Modularity (M), Smallworld index (σ), Hierarchy (β). Local measures include Betweenness Centrality (BC), Degree Centrality (DC), Participation Coefficient (PC), Nodal Local Efficiency (NLE) and Nodal clustering Coefficient (NCC). These measures are discussed below.

3.9.1 Assortativity

The Assortativity (r) is also known as assortative mixing and is a network property that measures the preference of nodes in a network to connect to others that are similar to them in some way. It is the correlation between the degree of a node and the average degree of the node's neighbors. A positive correlation indicates an assortative network, whereas a negative correlation indicates a disassortative network. Disassortative networks indicate strong hierarchical configurations.

$$r = \frac{m^{-1}\sum_i j_i \cdot k_i - \left[m^{-1}\sum_i 0.5(j_i + k_i)\right]^2}{m^{-1}\sum_i 0.5(j_i^2 + k_i^2) - \left[m^{-1}\sum_i 0.5(j_i + k_i)\right]^2} \tag{3.1}$$

j_i and k_i represent the degrees of the vertices j and k connecting the i^{th} edge, with i = 1,2, ..m; where m is the total number of edges.

3.9.2 Network efficiency

The Network efficiency ($E_{global}(G)$) is defined as the average inverse shortest path length in a network. Network efficiency for network G is as follows. Network efficiency measures quantify the efficiency of information transmitted across a network.

$$E_{\text{global}}(G) = \frac{1}{N(N-1)} \sum_{a \neq b \in G} \frac{1}{L_{ab}} \tag{3.2}$$

L_{ab} is the shortest path between nodes a and b in the network G. N is the total number of nodes in the network.

3.9.3 Modularity

The Modularity (Q) is a statistic used to distinguish between the number of intra-module connections of an existing network and randomly connected edges in a random network; it tells us how good the clustering is. Modularity is a measure of the degree to which a network can be divided into non-overlapping subgroups based on the connections between nodes. The modularity index measures the difference between the number of edges within communities and the expected number of edges in a null model where edges are placed at random while

preserving the network's degree distribution [24]. Modularity is computed based on a greedy agglomerative method [13]

$$Q = \frac{1}{2m} * \sum_{ij} (a_{ij} - \frac{(k_i * k_j)}{2 * m}) * \delta(\sigma_i, \sigma_j) \tag{3.3}$$

Where a_{ij} is the adjacency matrix of the network, k_i and k_j are the degrees of nodes i and j, m is the total number of edges in the network and (j,j) is the Kronecker delta function that takes the value 1 if nodes i and j belong to the same community (i.e., have the same community assignment) and 0 otherwise.

3.9.4 Small world index

The Small World Index is defined as the ratio of normalized clustering coefficient and normalized characteristic path length. A Small-world network has high clustering and short path lengths.

$$SWI(\sigma) = \frac{\gamma}{\lambda}; \gamma = \frac{CC}{CC_{\text{rand}}}; \lambda = \frac{CPL}{CPL_{\text{rand}}} CPL_{\text{rand}} = \frac{\sum_i \sum_j L_{ij}}{N \cdot (N-1)} \tag{3.4}$$

CC and CPL are the clustering coefficient and characteristic path length of the actual brain network, whereas CC_{rand} and CPL_{rand} are generated using 100 random networks by the Markov-chain algorithm. Here L_{ij} is the shortest path between node i and node j.

3.9.5 Hierarchical Coefficient

The hierarchical coefficient (β) quantifies the presence of the hierarchical organization in a network. It is a measure of the extent to which a node in a network is connected to nodes of higher or lower degree.

$$\beta = \frac{2m - 3k}{(k-1)^2} \tag{3.5}$$

where m is the number of connections in the network, and k is the degree of the measured node. (β) close to 1 indicates that the node is connected to other nodes of a higher degree, while (β) close to 0 indicates that the node is connected to other nodes of similar or lower degree.

3.9.6 Synchronization

The Synchronization is defined as the ratio of the second smallest Eigenvalue to the largest Eigenvalue obtained through the coupling matrix of a network G.

3.9.7 Betweenness Centrality

The Betweenness Centrality of a node (v) is defined as the ratio of the number of shortest paths passing through the node between any two given nodes $\sigma_{ab}(v)$ to the total number of shortest

paths between the two given nodes is σ_{ab}. If the betweenness centrality is high, it means the information flow through that node is high.

$$Bc(v) = \sum_{a \neq v \neq b} \frac{\sigma_{ab}(v)}{\sigma_{ab}} \tag{3.6}$$

3.9.8 Degree Centrality

The Degree Centrality of a node(v) is defined as the ratio of the degree of the node (d_v) to the maximum possible degree of the node. If the degree centrality of a node is high, it means it is more central. Nodes with a high degree of centrality are often considered to be crucial in the network as they have many connections and are potentially able to transmit information to a large number of other nodes.

$$Dc(v) = \frac{d_v}{(N-1)} \tag{3.7}$$

Where N is the total number of nodes in the network.

3.9.9 Participation Coefficient

The Participation coefficient of a node(v) reflects the within-module and intermodular communication.

$$P_c(v) = 1 - \frac{1}{N_s} \sum_{d=1}^{N_s} \left(\frac{d_{vs}}{d_v} \right)^2 \tag{3.8}$$

N_s is the number of modules, d_{vs} is the degree of a node 'v' to the nodes in module 's', d_v is the total degree of node ' V ' is 0 when there are no intermodular connections.

3.9.10 Nodal Local Efficiency

The Nodal local efficiency is a measure of the efficiency of information transfer between a node and its neighbors in a network. It is similar to network efficiency but computed in the neighborhood of a node. It is defined as the average inverse shortest path length between the node and its neighbors.

$$E_{\text{local}}(G) = \frac{1}{n-1} \sum_{a \neq b \in G} \frac{1}{L_{ab}} \tag{3.9}$$

L_{ab} is the shortest path between nodes a and b in the network G. n is the total number of neighbors of node 'a' in the network. The $E_{local(G)}$ values range from 0 to 1, where a value of 1 indicates that the node and its neighbors form a complete subgraph.

3.9.11 Clustering coefficient

The clustering coefficient of a node(v) is defined as the ratio of the number of connections between the neighbors of the node (e_v) to the total number of possible connections among (K_v) neighbors of the node. If the clustering coefficient of a node is high, it means the neighbors of the node are well connected. It measures the cohesiveness in a network.

$$N_{cc}(v) = \frac{2e_v}{K(v)K(v-1)} \tag{3.10}$$

The above graph measures also quantify network segregation (Nodal clustering coefficient, Nodal local efficiency, small world index and modularity), network integration (Global efficiency, assortativity and participation coefficient) and node centrality (Betweenness Centrality and Degree centrality) [38].

3.10 Statistical Methods

3.10.1 Spearman Rank Correlation

When it comes to understanding relationships between variables, correlations are one of the most widely used statistical measures. Among the various types of correlation coefficients, the Spearman rank correlation coefficient is a commonly used method to measure the strength and direction of the relationship between two variables. The Spearman rank correlation, also known as Spearman's rho or Spearman's rank correlation coefficient, is a non-parametric measure of correlation between two variables. It is a measure of the monotonic relationship between the two variables. It works by assigning ranks to the values of the two variables being compared. The ranks are then used to calculate the correlation coefficient, which ranges from -1 to 1. A correlation coefficient of -1 indicates a perfect negative correlation, 0 indicates no correlation, and 1 indicates a perfect positive correlation. Unlike other correlation coefficients, the Spearman rank correlation does not assume that the relationship between the variables is linear or that the variables follow a normal distribution. It is also robust to outliers and does not assume a linear relationship between the variables.

$$\rho = 1 - \frac{6\sum_{i=1}^{n}(d_i)^2}{n \cdot (n-1)^2} \tag{3.11}$$

Where d_i is the difference between the two ranks of each observation and n is the total number of observation

3.10.2 Pearson Correlation

The Pearson correlation, also known as the Pearson product-moment correlation coefficient, is a statistical measure that quantifies the relationship between two variables. This coefficient

is widely used in social sciences, economics, and engineering to understand the strength and direction of a linear relationship between two variables. Pearson correlation is a measure of the linear association between two continuous variables. The value of the correlation coefficient ranges from -1 to 1. If the correlation coefficient is positive, it indicates a positive linear relationship between the two variables, while a negative coefficient indicates a negative relationship. A correlation coefficient of 0 indicates no relationship between the two variables. It can be used to identify the strength and direction of a linear relationship between two variables and is not affected by the scale of measurement of the variables.It can only measure linear relationships between two variables. It assumes that the relationship between the two variables is symmetric and is sensitive to outliers and can be affected by them.

$$r = \frac{\sum_{i=1}^{n}(x_i - \bar{x})^2 \cdot (y_i - \bar{y})}{\sqrt{\sum_{i=1}^{n}(x_i - \bar{x})^2 \cdot \sum_{i=1}^{n}(y_i - \bar{y})^2}} \tag{3.12}$$

Where x_i value of the i_{th} observation of the first variable x, and x is the mean of the first variable x. y_i value of the i_{th} observation of the first variable y, and y is the mean of the first variable y.

3.10.3 Mann-Whitney-U test

One of the most common tests used in nonparametric statistics is the Mann-Whitney U test, which is also known as the Wilcoxon rank-sum test. This test is used to compare two groups and determine whether there is a significant difference between them. It assumes that the two groups are independent, the observations in each group are needed to be independent and identically distributed, and the dependent variable is ordinal or continuous. It also assumes homogeneity of variances across the two groups. It is a nonparametric test that does not require the data to be normally distributed. It is a robust test that is not affected by outliers or extreme values. The p-value obtained from the Mann-Whitney U test is compared to the significance level (alpha) to determine whether to reject or fail to reject the null hypothesis. If the p-value is less than alpha, the null hypothesis is rejected, and it can be concluded that there is a significant difference between the two groups. If the p-value is greater than alpha, the null hypothesis is failed to reject, and it can be concluded that there is no significant difference between the two groups.

$$U1 = \frac{n1 \cdot (n1+1)}{2}; \quad U2 = \frac{n2 \cdot (n2+1)}{2}; \quad U = U1 + U2 \tag{3.13}$$

The smallest among U1 and U2 is used for generating P-value. n1 and n2 are the sample sizes of two groups, respectively

3.10.4 Benjamini-Hochberg Correction

The Benjamini-Hochberg correction is a statistical procedure used to control for the false discovery rate (FDR), which is a type of error that occurs when a statistical test incorrectly identifies

a null hypothesis as significant in multiple testing situations. It is named after its inventors, Yoav Benjamini and Yosef Hochberg. This correction is widely used in the field of genomics and other areas of biomedical research, where large-scale hypothesis testing is common. The Benjamini-Hochberg correction is a procedure used to control for FDR in multiple testing situations. It is a step-up method that involves ranking all the p-values obtained from the statistical tests and comparing them to a threshold value. The threshold value is determined by a false discovery rate (FDR) threshold, which is usually set to 0.05 or 0.01. The Benjamini-Hochberg correction works by computing the critical p-value, which is the p-value threshold at which the FDR is equal to the specified FDR threshold. The critical p-value is then used to determine which hypotheses are significant and which are not.

$$\text{Critical Pvalue} = \left(\frac{\text{rank of } P_{valueTotal}}{\text{number of Tests}}\right) \times \text{FDR} \tag{3.14}$$

3.11 Independent Component Analysis

The Independent Component Analysis is a statistical technique used for separating a multivariate signal into independent, non-Gaussian components. In other words, ICA allows us to decompose a complex signal into simpler and more interpretable components. ICA finds a linear transformation of the data such that the transformed variables are statistically independent. This is achieved by assuming that the sources are non-Gaussian and that they are mixed linearly. Formally, let x be a d-dimensional observed vector, and let A be a d×d matrix that represents the mixing process. The goal of ICA is to find a matrix W such that the transformed variables $y = W_x$ are statistically independent. The matrix W is the inverse of the mixing matrix A, that is, $W = A^{-1}$.

3.11.1 Fast-ICA

The ICA algorithm is computationally expensive for high-dimensional datasets, and several fast ICA algorithms have been proposed to address this issue. One such algorithm is the FastICA algorithm, which is based on the concept of non-quadratic optimization. The FastICA algorithm uses a contrast function to measure non-Gaussianity and iteratively updates the weights until convergence.

The contrast function used in the FastICA algorithm with the tanh nonlinearity is given by:

$$G(y) = \tanh(\beta y) \tag{3.15}$$

where y is the output of the mixing matrix multiplied by the observed data, and β is a parameter that controls the shape of the tanh function.The FastICA algorithm with the tanh contrast function can be summarized in the following steps:

(a) Compute the output y = W_x, where x is the whitened data.

(b) Compute the contrast function G(y) and its derivative $g(y) = (1 - tanh^2(y))$.

(c) Update the weight matrix using the formula:

$$W_{new} = E[G(y)y^T] - E[g(y)]W_{old} \tag{3.16}$$

where E[·] denotes the expectation operator, and W_{old} is the weight matrix from the previous iteration.

(d) Orthogonalize the weight matrix using the Gram-Schmidt orthogonalization procedure.

(e) Repeat steps a-d until convergence

3.11.2 Minimum Description Length

One way to estimate the number of sources in ICA is to use the Minimum Description Length (MDL) criterion, which selects the model that provides the least coding length among a set of candidate models. The MDL criterion can be derived using information theory. The basic idea is to encode the data using a model that assumes N independent components and to compare the length of the encoded data with the length of the data itself. The MDL criterion balances the goodness of fit of the independent component to the data with the complexity of the independent component. The MDL criterion for ICA can be derived as follows. Let X be a mixed signal of T observations, where each observation is a linear combination of K independent components:

$$\mathrm{X} = \mathrm{W}^* \ \mathrm{S} + \mathrm{E}$$

where W is a K-by-K mixing matrix, S is a K-by-T matrix of independent components, and E is a K-by-T matrix of errors. The goal of ICA is to estimate the independent components S and the mixing matrix W from the observed signal X. The MDL criterion for ICA can be expressed as the sum of the lengths of the encoded data, the mixing matrix, and the independent component, where the length is defined as the number of bits required to encode the object. The MDL criterion is given by:

$$\mathrm{MDL(K)} = \mathrm{L(\ data\ \mid\ model\ )} + \mathrm{L(W)} + \mathrm{L(S)}$$

where L (data|model) is the length of the encoded data given the model, L(W) is the length of the encoded mixing matrix, and L(S) is the length of the encoded independent component.

The length of the encoded data can be estimated using the Shannon entropy of the data, which measures the average amount of information required to encode each observation. The length

of the encoded data is given by:

$$\mathrm{L}(\text{ data } \mid \text{ model }) = \mathrm{T}^{*}\mathrm{H}(\mathrm{X} \mid \text{ model })$$

where H(X | model) is the entropy of the data given the model.

The length of the mixing matrix and the independent component can be estimated using the Kolmogorov complexity of the object, which measures the length of the shortest program that generates the object. The length of the mixing matrix and the independent component are given by: L(W) = C(W) L(S) = C(S) where C(W) is the Kolmogorov complexity of the mixing matrix and C(S) is the Kolmogorov complexity of the independent component. The MDL criterion can be simplified by using the following approximation:

$$\mathrm{MDL}(\mathrm{K}) \approx \mathrm{T}^{*}\mathrm{H}(\mathrm{X} \mid \text{ model }) + \left(\mathrm{K}\hat{}2 + \mathrm{K}\right) * \log(\mathrm{T})/2$$

where the first term represents the length of the encoded data and the second term represents the complexity of the model. The best estimate of the number of independent components K is the one that minimizes the MDL criterion:

$$\mathrm{K}^{*} = \mathrm{argmin}(\mathrm{K})\,\mathrm{MDL}(\mathrm{K})$$

By minimizing the MDL criterion, ICA can be used to uncover the underlying independent components of complex data sets, providing insights into the underlying structure of the data.

3.11.3 Multimodal Canonical Component Analysis (mCCA) + Joint Independent Component Analysis (jICA)

Figure 3.2 depicts the pipeline of our multimodal fusion analysis. The minimum description length (MDL) method (Li et al., 2007) was used to determine the amount of independent components (M) to preserve for each local graph metric in both fc-fMRI and tc-dMRI modalities. Next, mCCA analysis was performed on fc-fMRI and tc-dMRI to produce canonical variates ($CV_{fc-fMRI} and CV_{tc-dMRI}$) and canonical components ($CC_{fc-fMRI} and CC_{tc-dMRI}$) .$CC_{fc-fMRI} and CC_{tc-dMRI}$ were concatenated and subjected to joint ICA, yielding mixing profiles (MM),unmixing profiles (umm), stability indices (IQ), and independent component loadings (IC). MATLAB v. 2019b (23) was used to calculate the mCCA and jICA analyses with custom scripts and the ICASSO toolbox (24). Effective mixing profiles were calculated for group comparisons using the following equations:

$$emm_{fc-fMRI} = [MM] \times CV_{fc-fMRI};\ emm_{tc-dMRI} = [MM] \times CV_{tc-dMRI} \tag{3.17}$$

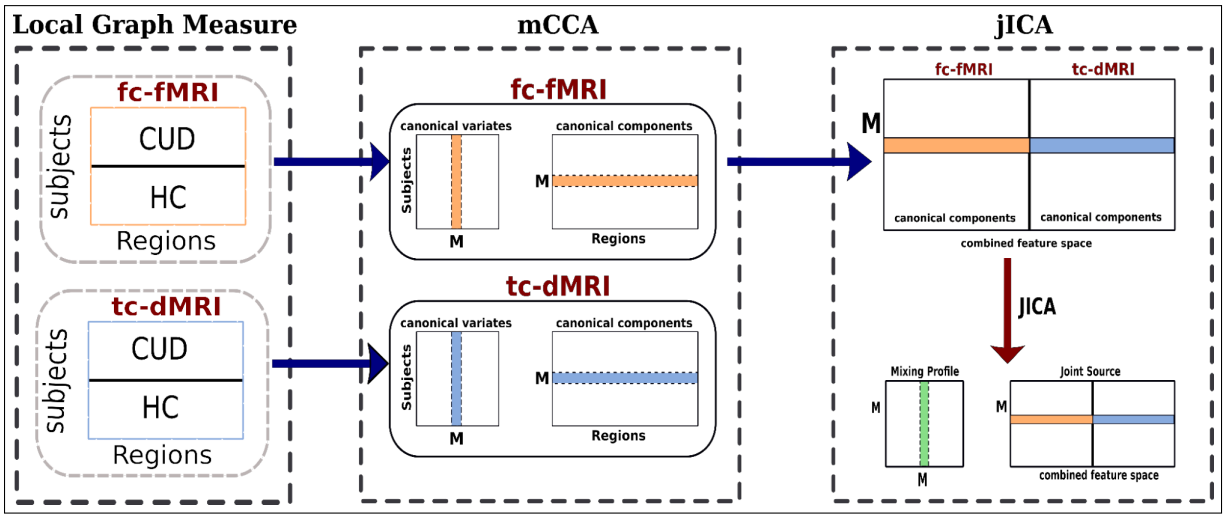

Figure 3.2 Workflow of the 2-way multimodal fusion

Chapter 4

Unimodal Analysis

The Unimodal analysis was performed to investigate brain network differences from the perspective of each modality (fc-fMRI and tc-dMRI). Global and local graph measures were analyzed to understand the functional and structural connectivity of the different brain regions. The global and local graph measures within each modality were tested for differences between CUD and HC using the Mann-Whitney-U test for independent two-samples. Spearman correlation between the graph measures and their corresponding clinical scores within each modality was performed. To account for multiple comparisons, we used FDR at 5% via the Benjamini-Hochberg procedure. R programming language version 4.1 was used for the statistical analysis. By performing unimodal analysis, we can gain insights into the underlying patterns and trends in our data and make informed decisions based on the results.

4.1 Threshold Averaged Global Graph measures

The average network measures across thresholds between 0.5%-50% (proportional) are computed using global signal regressed out rs-fMRI data, fMRI data without GSR and tc-dMRI data. The functional and structural connectome is computed using and Harvard Oxford Atlas. Figure 4.1 shows the graph-based global measures like Assortativity, Hierarchy, Modularity, Network Efficiency, Small World Index and Synchronization. In Figure 4.1.A the global graph-based measures are computed using rs-fMRI data without GSR with Harvard Oxford Atlas as the parcellation scheme. In 4.1.B the global graph-based measures are computed using rs-fMRI data with GSR with Harvard Oxford Atlas as the parcellation scheme.

Figure 4.2 shows the graph-based global measures like Assortativity, Hierarchy, Modularity, Network Efficiency, Small World Index and Synchronization. All the global graph-based measures are computed using tc-dMRI data with Harvard Oxford Atlas as the Parcellation scheme.

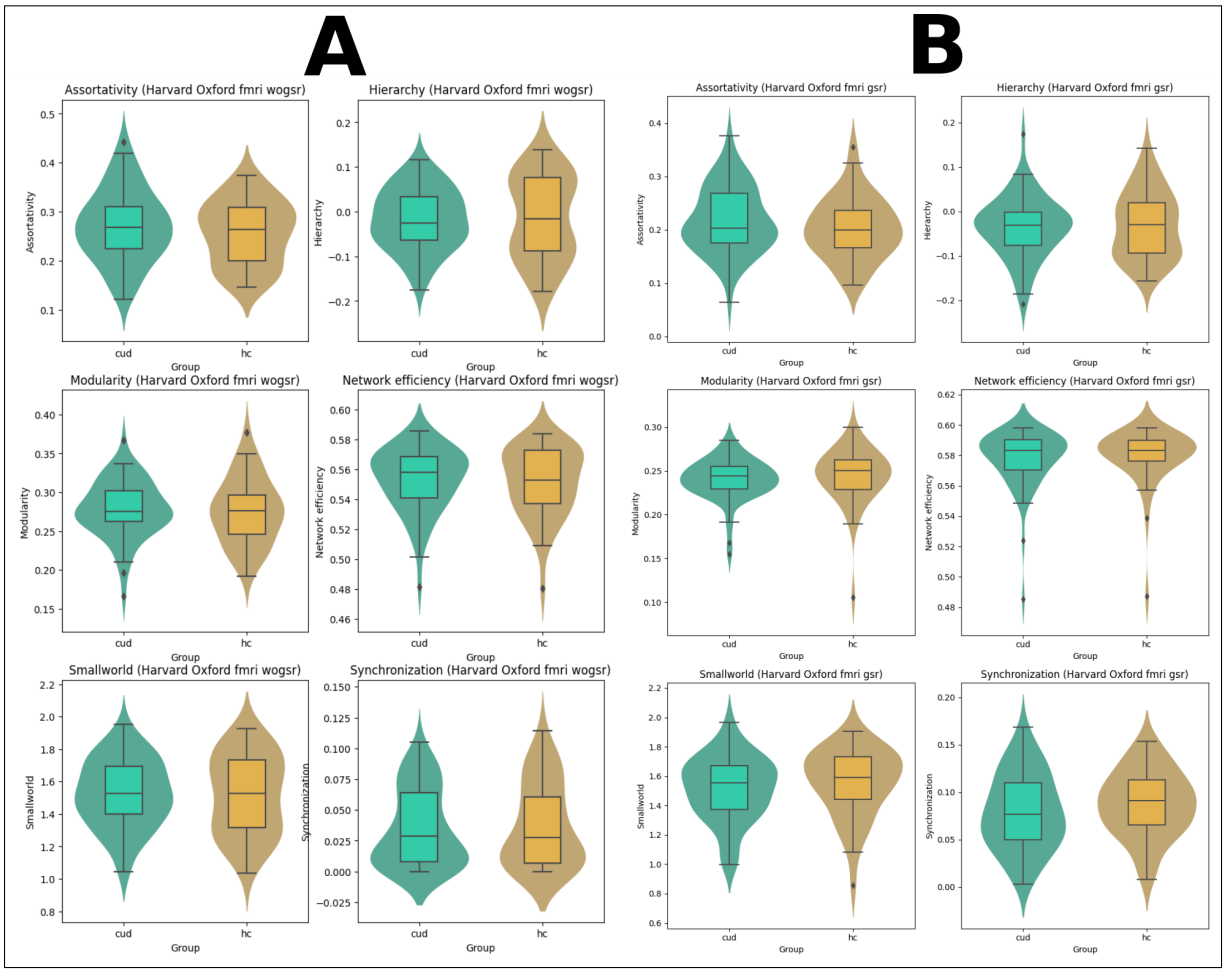

Figure 4.1 Graph-based global measures computed using rs-fMRI

4.1.1 Statistical Analysis

No significant differences were observed between CUD and HC groups for the global measures computed using Harvard Atlas in the fc-fMRI modality. For either modalities, there were no significant correlations between global graph measures and clinical scores.

4.2 Threshold Averaged Local Graph measures

Local graph measures, such as Betweenness Centrality, Participation Coefficient, Nodal Local Efficiency, Nodal Clustering Coefficient, and Degree Centrality, are calculated using the same thresholds utilized in determining the global graph measures. No significant differences were observed between CUD and HC groups for the global measures in the tc-dMRI modality. On the other hand, only the left Caudate exhibited a significant decrease in Participation Coefficient

among CUD compared to HC in the fc-fMRI modality (U =1880, p=0.0027, p_{fdr}=0.030) (Refer Figure 4.3).No significant correlations were observed between local graph measures and their corresponding clinical scores.

4.3 Summary of Unimodal Analysis

Unimodal analysis of the fc-fMRI modality revealed that individuals with cocaine use disorder (CUD) had a reduced contribution of the left caudate to inter-modular communication compared to the healthy control (HC) group. The caudate nucleus, which is part of the striatum, is known to play a crucial role in habit learning, motor behavior, and compulsive drug-seeking behavior. The reduced inter-modular communication of the caudate nucleus in individuals with CUD may contribute to their compulsive drug-seeking behavior.

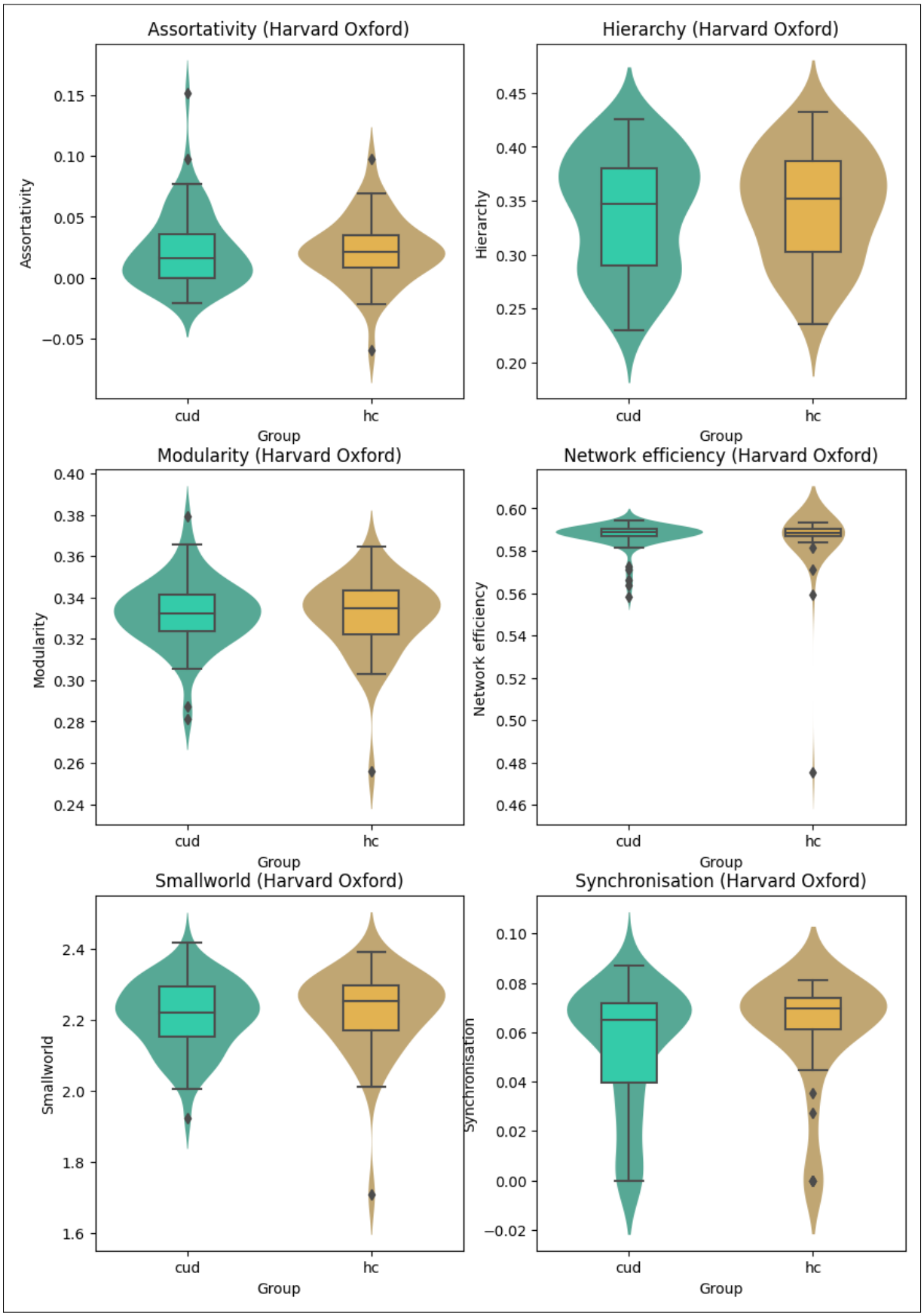

Figure 4.2 Graph-based global measures computed using tc-dMRI

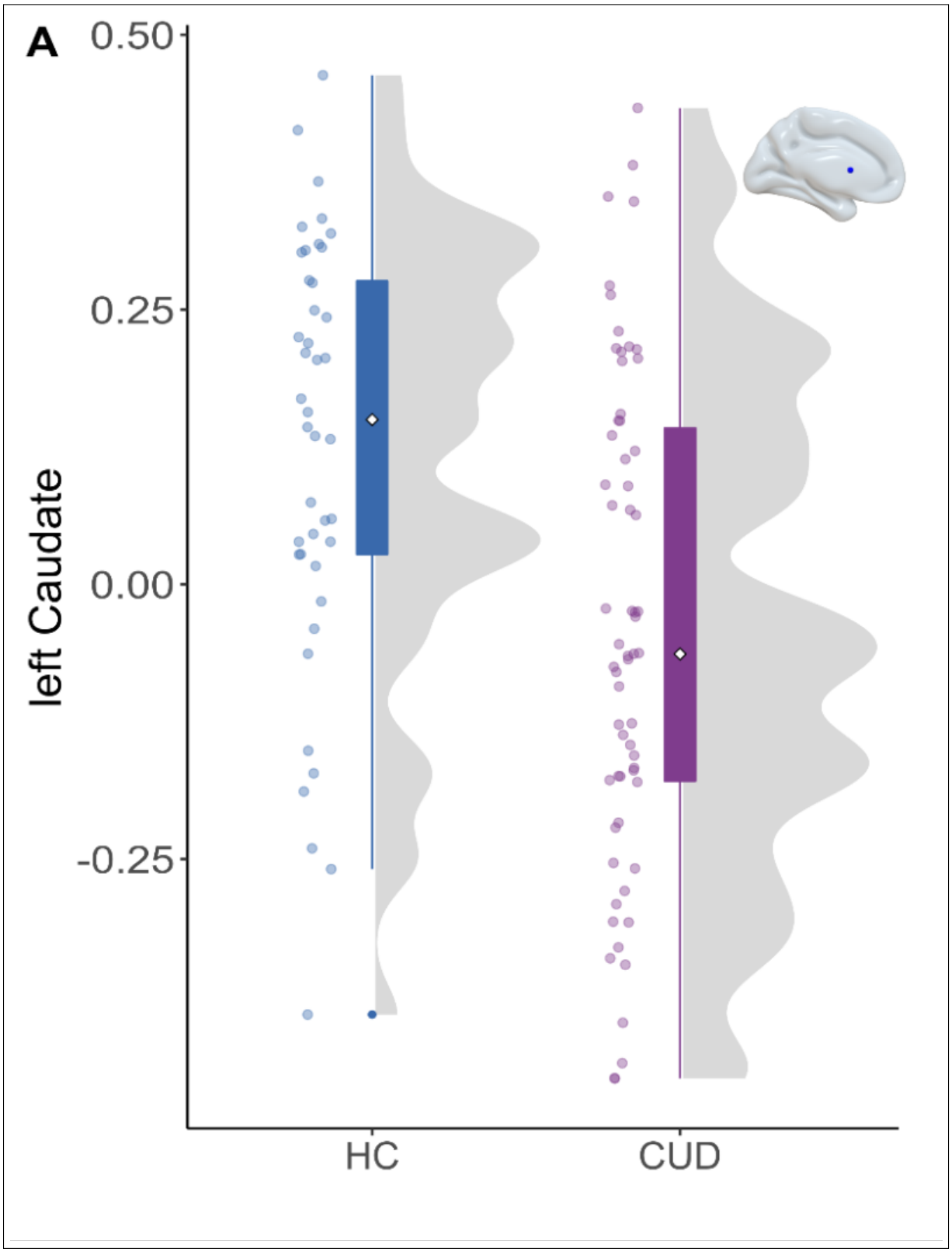

Figure 4.3 Group comparison of Participation Coefficient from unimodal analysis, significant on left Caudate.

Chapter 5

Multimodal Analysis

Sui et al, [59] outline several multimodal fusion methods and divide them into three different categories based on their objectives: finding flexible connections between modalities, separating sources and discovering the common mixing profiles, and examining both flexible modality connections and distinct sources. The several outlined blind source separation methods were evaluated by simulating their performances on a generated dataset of 100 noisy (random Gaussian noise was added) images with fMRI and EEG signals as the two modalities. Based on various metrics, it was evident that jICA and mCCA are good at source separation and modality associations, respectively. Whereas, mCCA+jICA had more reliability in estimating the modality relations (high or low correlations) along with good source separation and robustness to noise. Hence, our multimodal fusion analysis was performed using the above-mentioned approach, that is, mCCA+jICA.

5.1 Multimodal Fusion

Our multimodal fusion analysis pipeline is illustrated in Figure 3.2. Age was regressed out from the local graph-based measures calculated for each modality. Prioritizing age as a covariate is grounded in its established significance in literature [73]. Notably, the dataset lacked complete information on sex, education and average consumption per intake varied, necessitating the use of imputation, which introduces a potential bias. Furthermore, the age range of participants, spanning from 18 to 50 for individuals with Cocaine Use Disorder (CUD) and 18 to 48 for the Healthy Controls (HC), rationalizes the decision to regress out the influence of age. The minimum description length (MDL) for each local graph metric is as follows: $M_{BC} = 4, M_{DC} = 10, M_{NCC} = 13, M_{NLE} = 19, M_{PC} = 9$; in both fc-fMRI and tc-dMRI modalities. All ICs values were normalized to Z-scores. In order to investigate regions with the highest contribution for the mixing profiles, we used a threshold of Z$\pm$ 2.3. The effective mixing profiles ($emm_{fc-fMRI}$ and $emm_{tc-dMRI}$) of those ICs with an IQ > 0.8 were considered. Based on the previous

research [1], these mixing profiles were further correlated with each other along with their corresponding clinical measures using Spearman correlation. Mann–Whitney–Wilcoxon test for independent two-samples was computed to reveal group differences between CUD and HC for each $emm_{modality}$. All results were corrected for multiple comparisons using FDR (Benjamini-Hochberg) at 5%.

5.2 Results

The local graph measures of integration, betweenness centrality (BC), and participation coefficient (PC), had IQ > 0.8, resulting in one IC in the case of BC (IC2) and two for PC (IC1 and IC4). Only the fc-fMRI modality showed significant group differences, with BC (p_{value}=0.028, p_{fdr}=0.042) having greater values in the CUD sample and PC (p_{value}=0.026,p_{fdr}=0.042) having lower values in the CUD sample. In fc-fMRI modality, the significance of the BC (IC2) suggests that the independent component was expressed more strongly in the CUD group compared to the HC group, thus resulting in a lesser number of shortest pathways via nodes (Table 5.1). For PC, the independent component (IC4) that corresponds to the fc-fMRI modality was stronger in the CUD group than the HC, suggesting a higher level of node participation in their own communities (Table 5.2). The joint-IC2 of BC was characterized by the contributions of the left Temporal pole, left Middle Temporal gyrus and bilateral Anterior Cingulate gyrus in fc-fMRI modality along with bilateral Thalamus and bilateral Putamen in tc-dMRI modality (Table 5.2). In the tc-dMRI modality, the joint-IC4 of PC revealed significant connectivity in the left Parahippocampal gyrus and the right Occipital Fusiform gyrus, as well as the bilateral Posterior Cingulate gyrus, left Cuneal cortex, and bilateral Caudate in the fc-fMRI modality (Figure 5.1 and Table 5.2). it is to be noted that Figure 5.1 illustrates the regions that contribute to the joint independent components in fMRI modality for Betweenness Centrality and Participation Coefficient. For visualization purposes, we opted to include the regions contributing to the joint independent components tc-dMRI modality within Figure 5.1. It is important to acknowledge that, in contrast to fc-fMRI modality, these regions did not attain statistical significance in terms of group differences but demonstrated positive associations with the regions identified in the fc-fmri modality. Figure 5.2 depicts a positive correlation between the effective mixing profiles ($emm_{fc-fMRI}$ and $emm_{tc-dMRI}$) of joint IC2 and joint IC4 for BC and PC, respectively. This demonstrates a strong association between the regions that contribute to the joint independent component in both the fc-fMRI and tc-dMRI modalities for BC and PC. There were no significant correlations with the clinical measures.

Table 5.1 Group comparison in IC_n loadings (IQ > 0.8), median effective mixing profiles of CUD and HC and statistics of each graph metric

		IC	HC(n = 42)	CUD(n = 63)	Statistic	p value	p_{fdr}
Betweenness Centrality	fc-fMRI	IC_2	-0.0094	0.0088	$W = 987$	0.028^*	0.042^*
	tc-dMRI	IC_2	0.0006	-0.0001	$W = 1325$	0.992	0.992
Participation Coefficient	fc-fMRI	IC_1	-0.0111	-0.0112	$W = 1352$	0.852	0.852
		IC_4	0.0104	0.0027	$W = 1664$	0.026^*	$0.042*$
	tc-dMRI	IC_1	-0.0038	0.0018	$W = 1143$	0.24	0.720
		IC_4	-0.0015	-0.0011	$W = 1235$	0.567	0.850

Table 5.2 Regions in joint IC_n at Z± 2.3

			Anatomical regions	Z-score
Betweenness Centrality	fc-fMRI	IC_2	Left Temporal Pole	2.885
			Right Middle Temporal Gyrus, temporo-occipital	-2.92
			Right Cingulate Gyrus, anterior division	2.610
			Left Cingulate Gyrus, anterior division	3.684
	tc-dMRI	IC_2	Right Thalamus	-4.792
			Left Thalamus	-4.662
			Right Putamen	-3.957
			Left Putamen	-3.868
Participation Coefficient	fc-fMRI	IC_4	Right Cingulate Gyrus, posterior division	-2.340
			Left Cingulate Gyrus, posterior division	-2.321
			Left Cuneal Cortex	2.478
			Left Caudate	2.315
			Right Caudate	2.489
	tc-dMRI	IC_4	Left Parahippocampal Gyrus, anterior division	2.638
			Right Occipital Fusiform Gyrus	2.694

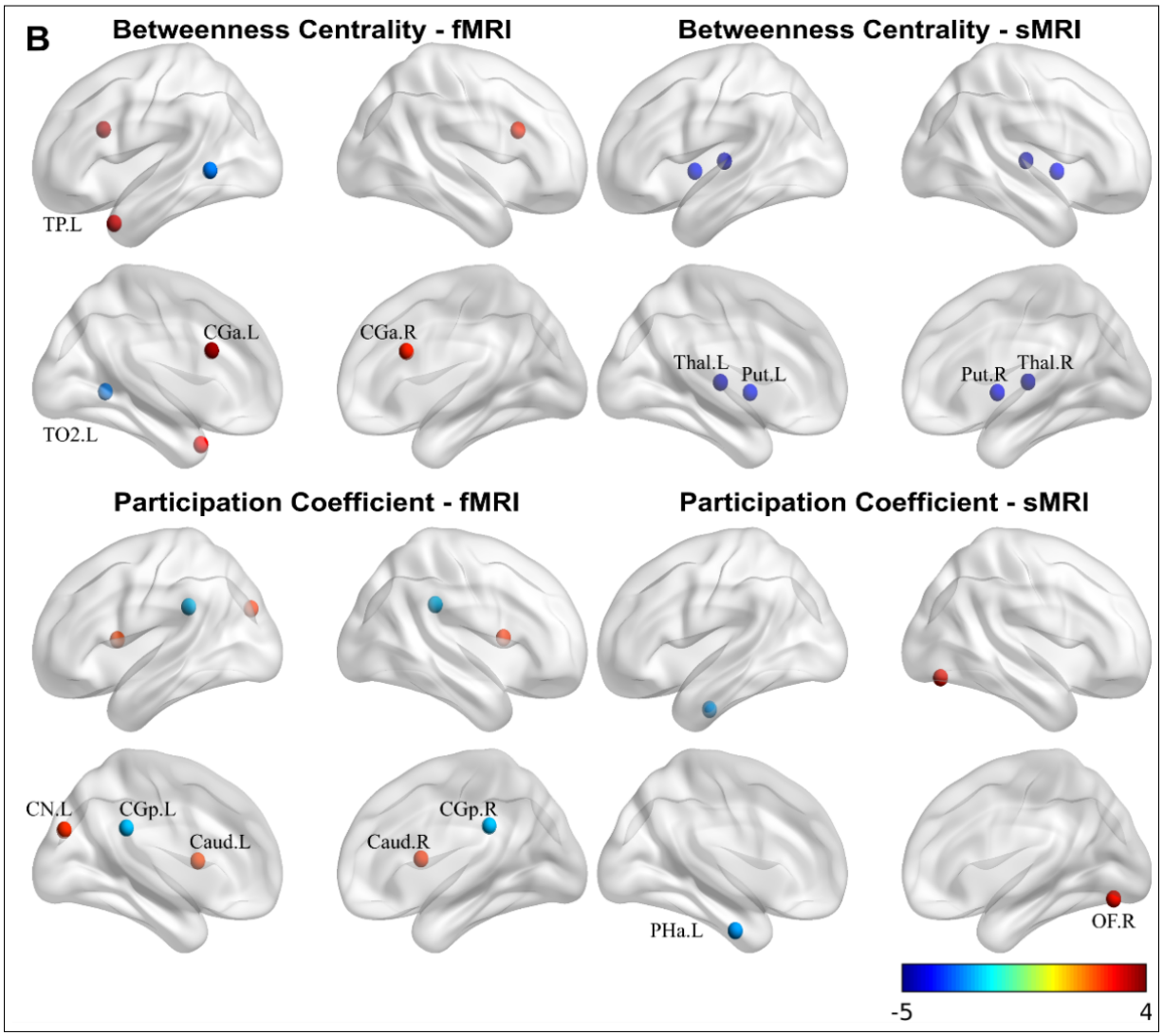

Figure 5.1 Multimodal group-discriminating BC-IC2 and PC-IC4. TP.L = left Temporal Pole, TO2.L = right middle Temporal gyrus, temporo-occipital, CGa.L = left Cingulate Gyrus, anterior division, CGa.R = right Cingulate Gyrus, anterior division, Thal.L = left Thalamus, Thal.R = right Thalamus, Put.L = left Putamen, Put.R = right Putamen, CGp.L = left Cingulate Gyrus, posterior division, CGp.R = right Cingulate Gyrus, posterior division, CN.L = left Cuneal Cortex, Caud.L = left Caudate, Caud.R = right Caudate, PHa.L = left Parahippocampal Gyrus, anterior division, OF.R = right Occipital Fusiform Gyrus.

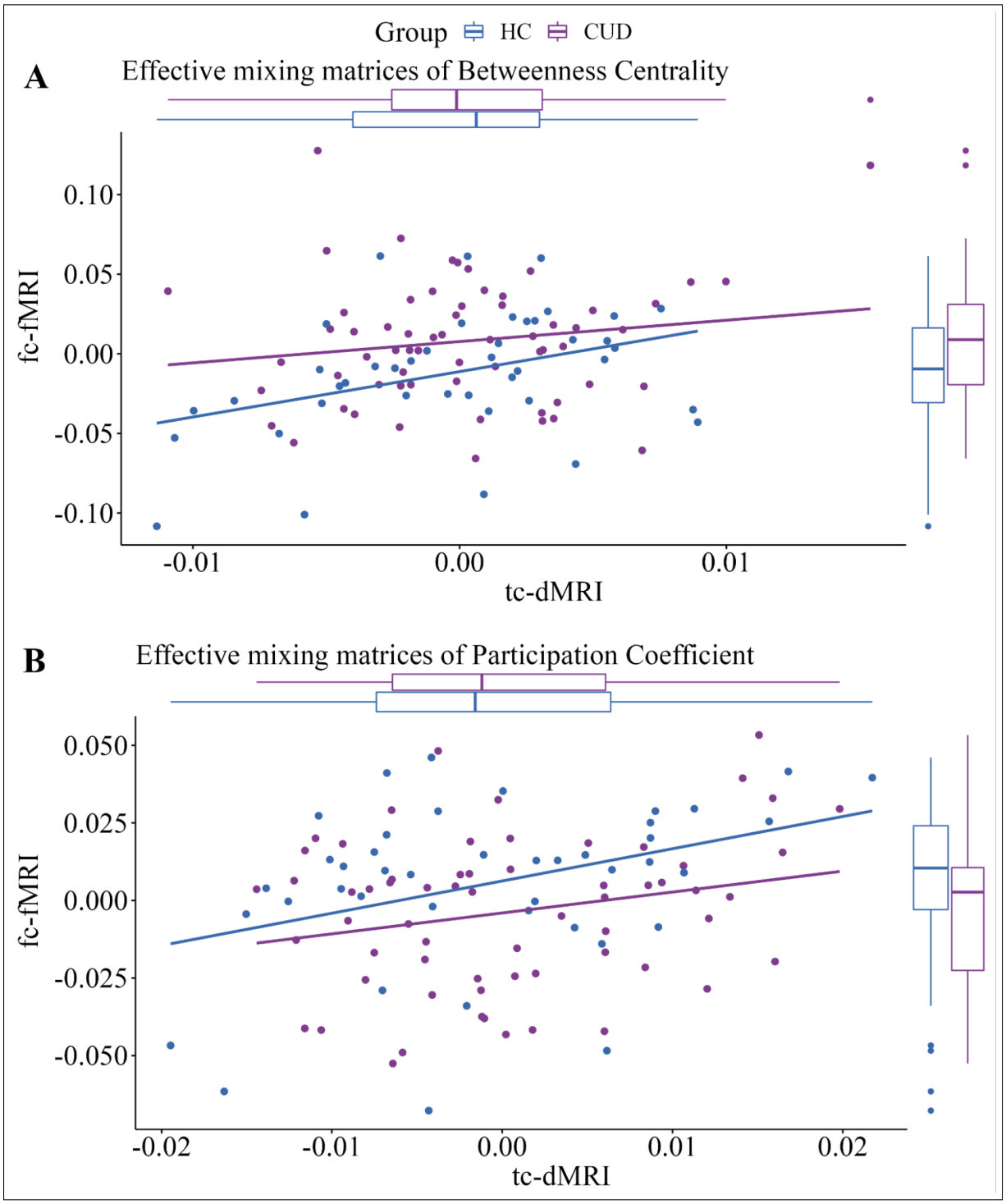

Figure 5.2 Association between effective mixing matrices of fMRI and dMRI Independent components. A) Association of emmfc-fMRI and emmtc-dMRI for betweenness centrality (BC IC2) with a significant correlation (r = 0.196, p_{fdr}r = 0.045), B) Association of $emm_{fc-fMRI}$ and $emm_{tc-dMRI}$ for participation coefficient (PC IC4) with a significant correlation (r =0.223, $p_{fdr} = 0.044$).

5.3 Summary of Multimodal fusion analysis

The results indicated that the BC and PC measures showed significant differences between the CUD and HC groups only in the fc-fMRI modality. BC had higher values in the CUD sample, while PC had lower values. This suggests that the independent component associated with BC was more pronounced in the CUD group, resulting in fewer shortest pathways via nodes. On the other hand, the independent component linked to PC was stronger in the CUD group, indicating a higher level of node participation in their own communities. Furthermore, a positive correlation was observed between the effective mixing profiles of joint BC and joint PC in fc-fMRI and tc-dMRI modalities. This indicates a strong association between the regions contributing to the joint independent component for BC and PC. Overall, the multimodal analysis revealed that individuals with CUD exhibit altered brain connectivity patterns compared to healthy individuals, particularly in terms of betweenness centrality and participation coefficient measured through fc-fMRI. These findings provide insights into the neural mechanisms underlying CUD and may contribute to a better understanding of the disorder.

Chapter 6

Conclusion

In this study, we examined the macroscopic network-based differences using graph theory, between patients with cocaine use disorder (CUD) and matched healthy controls (HC) by combining fc-fMRI and tc-dMRI imaging modalities. While multimodal fusion has been carried out in other studies, to our knowledge, this is the first multimodal-fusion study that uses graph theory to explore topological alterations in CUD patients. First, we evaluated the differences between the two groups in functional and structural modalities separately. Subsequently, we performed a multimodal fusion of fc-fMRI and tc-dMRI modalities, which enabled us to understand network patterns conveyed by both modalities, leveraging a well-defined mathematical framework (i.e. graph theory). While this study was exploratory in nature, post rigorous multiple comparison corrections, our study identified brain regions that not only agrees with earlier studies but also revealed interesting observations that may contribute to a better understanding of CUD patients. We found impairment in inter-module communication (i.e., participation coefficient) in CUD in individual and joint modalities. However, impairment in internode information communication was observed in CUD only in joint modalities. These results demonstrate the utility of multimodal fusion in unearthing latent network patterns which would otherwise be lost if done separately.

Unimodal analysis indicated a reduced contribution of left caudate to inter-modular communication among the CUD when compared to HC in the fc-fMRI modality. The caudate nucleus, a part of the striatum, has been described as a core region involved in habit learning, motor behavior, and compulsive drug-seeking behavior [32]. This structure is the major integration site of the cortico-basal ganglia-thalamic circuit in which psychostimulants such as cocaine induce cellular, molecular and connectivity adaptations through the shifting of the predominance of neuronal signaling, leading to the continued drug use [72]. The present findings are in line with previous MRI studies which have found striatum alteration in CUD patients such as a reduced striatal volume [5] [47], morphological and microstructural changes [19][53], and altered

functional connectivity[74] [23]. A lower inter-modular communication of the caudate nucleus in CUD may be related to compulsive drug-seeking behavior.

Similar to our results, modeling pairwise relations between brain regions using topological metrics in CUD patients has not been as clear to unravel network structure damage [75] [69] [10]. However, using graph-theory-based multimodal fusion analysis, we found other subcortical regions appearing in addition to the caudate nucleus found in the unimodal analysis. The joint components involved subcortical nodes such as the putamen and thalamus, as well as in cerebral cortex such as the anterior/posterior cingulate, parahippocampus, medial temporal, occipital fusiform gyrus, and cuneal cortex, which are commonly associated with CUD [27] [50].

Brain networks of CUD patients revealed a lesser number of shortest pathways via nodes, reflected by higher betweenness centrality (BC) in fc-fMRI modality (i.e. the contribution rate of nodes in the information interchange with other nodes). This could be understood better by taking into account the structural connectivity, as previously suggested by Ma et al., (2015) [34], Pacheco et al.[45], and described by Meade et al., (2021) [37]. A lower BC was observed in the Temporo-occipital part of the middle temporal gyrus (TO2) in CUD, a region related to multimodal sensory integration [39] and cognitively implicated in the organization of communicative information [48], emotion recognition, empathic arousal, and retrieval of relevant schemas (i.e. moral judgments) [18]. This region has also been shown to be impaired in CUD [53][8] and associated with cue reactivity/craving in cocaine and other SUDs [11][61][65] [71]. Regular cocaine abuse could negatively affect cognitive processing as well as high-level socio-affective processes (i.e. moral judgments) that could lead to insensitivity toward negative stimuli and antisocial behaviors [6].

On the other hand, the disruption of the bilateral anterior cingulate gyrus (ACC) in terms of connectivity has been extensively observed in CUD patients [11][61][65] [71] [6] [58]. In recent years, ACC is considered one of the main potential biomarkers and targets for brain stimulation treatments, such as repetitive transcranial magnetic stimulation, due to the strong structural and functional connectivity with the reward system and executive-salience networks [67] [76]. As reflected by our results, the disturbances in the communication of this region could lead to the reorganization of brain networks observed in CUD [76]. Overall, the higher BC observed in certain regions of CUD patients could be indicative of an alteration in the organization of the functional networks. While the unimodal analysis did not reveal these functional changes, the multimodal analysis resulted in identifying these alterations.

Although there have been few studies that have investigated the role of brain regions in inter-network communication particularly, it is noteworthy that we found a lower participation coefficient (PC) in the caudate nucleus among the CUD when compared to HC in both unimodal and multimodal analyses. The reduced participation coefficient displayed by the caudate nucleus along with the posterior cingulate cortex (PCC) (internally oriented processing), an important

region of the default mode network, suggests a reduced role they both play in inter-module information transfer in CUD when compared to HC. Previously, Liang et al.[29] reported a lower PC of both anterior and posterior cingulate cortex in CUD, and connected with regions associated with executive control network (externally oriented executive functioning), explaining the cognitive difficulties in these patients they also found a close connection of the caudate nucleus over different brain networks altered in CUD [29][38]. Several studies have highlighted both regions as critical hubs vulnerable to cocaine misuse and other SUDs [62][56]. One of the main reasons may be the high metabolic costs involved in the process of integration and information exchange within brain networks, both implicated and affected not only in SUD pathology, but also in Alzheimer's-type neurodegeneration, dementia and depression [29].

Employing graph theory analysis in a multimodal setting offered profound insights into the connectivity changes. Previously, Schweitzer et al.[57] observed that individuals with prenatal drug exposure (PDE) displayed lower global efficiency and a tendency towards reduced local efficiency, particularly in the middle frontal gyrus (MFG). Additionally, Wang et al. [69] used graph theoretical analysis to examine the Functional Connectome (FCM) in polydrug users, primarily cocaine-dependent, finding enhanced functional connectivity across various brain regions but decreased communication efficiency and diminished small-world characteristics. This indicates a compromise in standard inter-regional communications and topology. Pacheco et al. [45] demonstrated that in individuals with Inhaled Substance Abuse Disorder (ISAD), there is an increase in BC across various subnetworks. Although the above studies employ unimodal methodologies, their insights are instrumental in corroborating findings from the multimodal fusion of graph-based measures. Our study showed an increased BC in several brain regions in CUD patients, which aligns with the existing literature. Overall, These results might indicate that the structural organization of the network, which underlies functional connectivity networks, is altered. It is also evident that in substance abuse scenarios, the brain prioritizes function, albeit with lessened efficiency. We can potentially conclude that nodes or brain regions begin to play a more diffused and less efficient role in information communication and functioning in disorders, especially in the case of substance abuse.

6.1 Limitations

Despite the findings, there are two main limitations in the present study. The first one is the missed significance in tc-dMRI independent components and the other limitation is related to the lack of correlation with clinical metrics. The no-group differences in the tc-dMRI modality were observed in unimodal or multimodal analyses, which could be attributed to metrics based on graph theory, which are used to detect higher-order relationships in the brain. In both unimodal and multimodal analyses, these higher-order dependencies were manifested as distinct functional differences. Furthermore, this could also explain the lack of correlations with clinical

measures. In addition, the existence of a subclinical and/or cognitive profile within the CUD group could also explain the lack of correlations with clinical measures. Since our aim is to investigate broader patterns of connectivity across large brain regions with better granularity we performed all the analyses using Harvard Oxford atlas. The choice of a specific parcellation scheme influences the identification of connections, characterization of functional networks, and insights into brain function and disorders. Furthermore, future studies can incorporate insights gained by comparing connectivity patterns derived from various parcellation schemes.

6.2 Conclusion

In summary, we found unimodal and multimodal cocaine impairment on inter-module communication and internode exchange communication only in a multimodal manner. Unimodal results show a striatal decrease of the participation coefficient, but the applied supervised data fusion could reveal other regions with cocaine-related impairments on joint-functional communication. Further research applying the combination of modalities, as in longitudinal protocols is needed to develop better pre-treatment/post-treatment intervention designs and to provide new insights into the neurobiological mechanisms of the SUDs.

Related Publications

1. Rasgado-Toledo, J., Duvvada, S. S., Shah, A., Ingalhalikar, M., Alluri, V., Garza-Villarreal, E. A. (2024). Structural and functional pathology in cocaine use disorder with polysubstance use: A multimodal fusion approach structural-functional pathology in cocaine use disorder. Progress in Neuro-Psychopharmacology and Biological Psychiatry, 128, 110862. https://doi.org/10.1016/j.pnpbp.2023.110862

Chapter 7

Supplementary Study

7.1 Seed-based Connectivity

In a previous study by Rasgado-Toledo et al.[53], we found white and gray matter pathology among interconnections between frontal hemispheres, frontal to parieto-temporal lobes and subcortical regions. In this study, we expanded the results by investigating variability in functional connectivity (FC) between regions identified with gray and white matter pathology in cocaine use disorder patients (CUD). We included 63 CUD patients along with 42 matched non-dependent healthy controls (HC), paired by age, sex, handedness and education, recruited as part of the SUDMEXCONN database see Angeles-Valdez et al. [3]. FC was computed using time-series data based on the Desikan Killiany Atlas. We performed the Mann-Whitney test for the identification of significant differences between groups. These were further checked using a non-parametric permutation test (10,000 permutations). Results revealed significantly greater FC between the right posterior cingulate (PCC) and postcentral gyrus for CUD than HC. Although this region is outside the commonly studied mesolimbic-cortical system, this is consistent with previous cocaine cue-craving-related task fMRI activations in PCC [14], and higher activations to inhibition tasks within the postcentral gyrus for patients with positive cocaine use [52]. We also found significantly decreased FC for CUD among several right hemispheric regions of the prefrontal, subcortical and cerebellum, suggesting a pathological network state. Interestingly, the higher connectivity between the PCC, a node of the default mode network, and the postcentral gyrus, the primary somatosensory cortex, may imply an increase in interoception possibly related to compulsive behaviour.

7.1.1 Connectivity Analysis

Functional connectivity was computed for selected regions based on the Desikan Killiany (86 regions). After an extensive literature survey, we identified 19 brain regions (refer table 7.1)

that showed significant differences in connectivity at the group level. At an individual level, for these 19 selected regions, the mean time series was extracted from each region, and the functional connectivity was estimated by computing all pairwise Pearson correlations. Subsequently, we performed a non-parametric statistical test of difference called the Mann-Whitney U test at the group level and identified significant group differences. We additionally estimated the significance of the observed differences via a non-parametric permutation test (10,000 permutations).

Results (Table 7.2) revealed that significantly greater connectivity was observed between the right Posterior Cingulate and right Postcentral is higher for CUD than HC. On the other hand, significantly decreased FC was observed between several right hemispheric regions for the CUD.

Figure 7.1 illustrates the connections between the node pairs that exhibited significant group differences. The lower connectivity between prefrontal, subcortical and cerebellum regions suggests a pathological network state. Interestingly, the higher connectivity between Posterior Cingulate Cortex, a node of the default mode network, and the PostCentral gyrus, the primary somatosensory cortex, may imply an increase in interoception possibly related to compulsion behaviour.

Table 7.1 Regions of Interest

Region of Interest	Abbreviation	MNI coordinates (X)	MNI coordinates (Y)	MNI coordinates (Z)
Left Lateral Orbitofrontal	l.Lateralorbitofrontal	-24.788431	28.715777	-16.968762
Left Middle Temporal	l.middletemporal	-57.751067	-30.2239	-13.290262
Left Parahippocampal	l.parahippocampal	-23.907604	-33.142327	-19.249481
Left ParsOpercularis	l.parsopercularis	-45.746763	14.555066	11.852166
Left ParsTriangularis	l.parstriangularis	-44.017232	30.266616	0.805347
Left rostral middle Frontal	rMFG-L	33.96575	42.836306	17.683447
Left superior frontal	l.superiortemporal	-53.401526	-15.660875	-4.006122
Right Inferior Parietal	IPG-R	44.34569	-61.781892	28.633137
Right Inferior Temporal	r.inferiortemporal	50.781852	-31.732182	-26.194109
Right LateralOrbitofrontal	LOC-R	24.236422	29.349355	-17.996568
Right ParsTriangularis	r.parstriangularis	46.623897	29.45939	3.342318
Right Post Central	PoG-R	42.365002	-22.476359	44.557213
Right Posterior Cingulate	pCg-R	5.685813	-17.196104	38.859022
Right rostral middle Frontal	rMFG-R	33.96575	42.836306	17.683447
Right Supramarginal	SMG-R	52.104994	-33.127594	31.196859
Left Thalamus	Thal-L	12	-18	9
Left Pallidum	Pall-L	21	-3	0
Right Cerebellum	Cerebellum-R	-24	-65	-48
Right Thalamus	Thal-R	-12	-18	9

Table 7.2 Pair-wise Mean Connectivity Differences

Node Pair(A-B)	**CUD**	**HC**	**P-value(Man Whitney)**	p_{fdr}**(Man Whitney)**
rMFG.L-Pall.L	0.134	0.240	0.0177	0.035
IPG.R -Thal.R	0.149	0.294	0.008	0.0267
LOC.R-SMG.R	0.311	0.402	0.0475	0.0475
LOC.R-Cerebellum.R	0.366	0.488	0.0075	0.0267
PoG.R-PCG.R	0.335	0.233	0.0271	0.0387
pCg.R-Thal.R	0.171	0.266	0.0424	0.0471
rMFG.R-Thal.R	0.170	0.278	0.0339	0.0424
Thal.L-Cerebellum.R	0.137	0.243	0.0248	0.0387
Pall.L-Cerebellum.R	0.114	0.235	0.0071	0.0267
Cerebellum.R-Thal.R	0.161	0.278	0.0126	0.0315

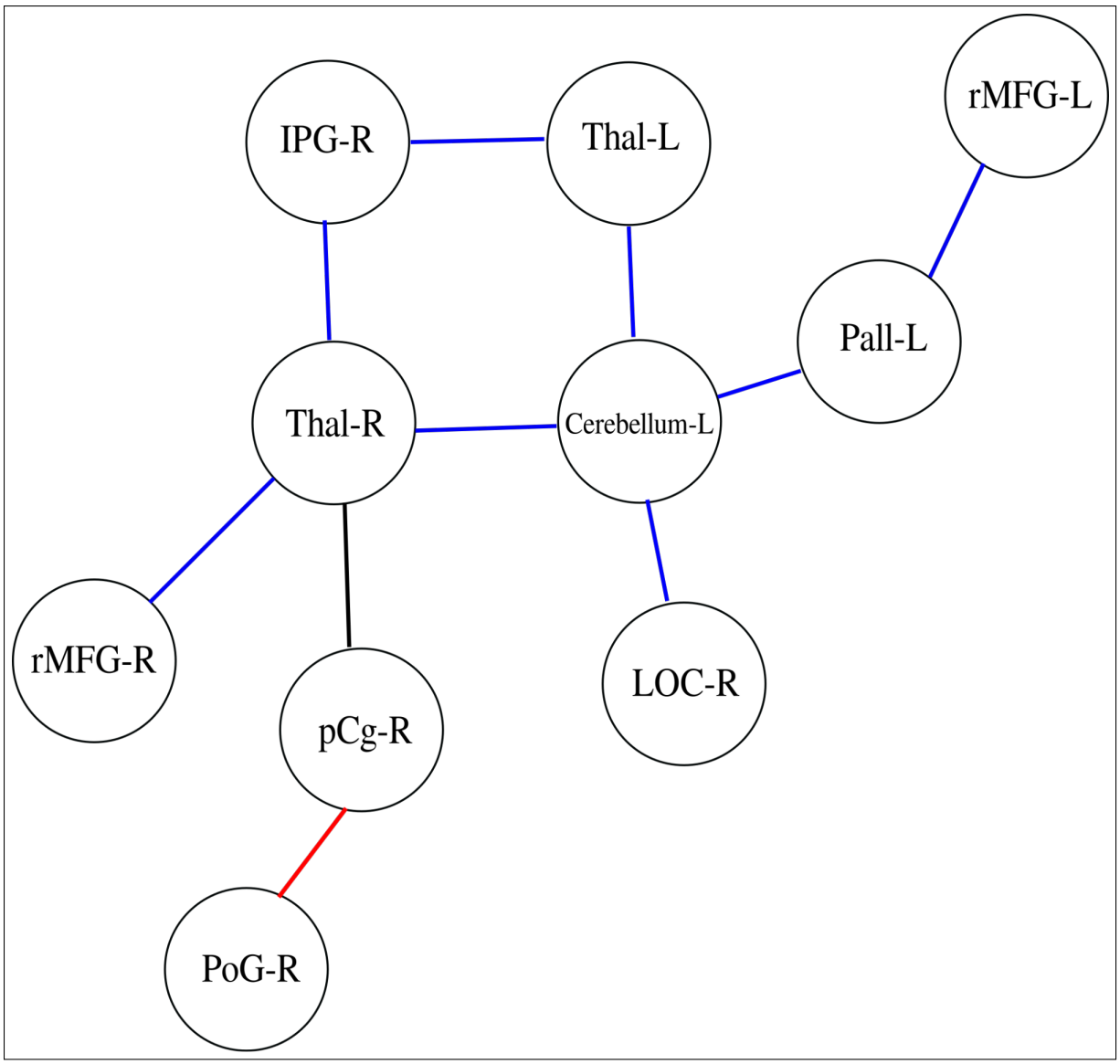

Figure 7.1 Seed-based Connectivity. The Black edge indicates a stronger connection in the HC whereas the red edge represents a stronger connection in CUD.

Bibliography

[1] A. Abrol, B. Rashid, S. Rachakonda, E. Damaraju, and V. D. Calhoun. Schizophrenia shows disrupted links between brain volume and dynamic functional connectivity. *Frontiers in neuroscience*, 11:624, 2017. 35

[2] N. Albein-Urios, J. Verdejo-Román, S. Asensio, C. Soriano-Mas, J. M. Martínez-González, and A. Verdejo-García. Re-appraisal of negative emotions in cocaine dependence: Dysfunctional corticolimbic activation and connectivity. *Addiction biology*, 19(3):415–426, 2014. 10

[3] D. Angeles-Valdez, J. Rasgado-Toledo, V. Issa-Garcia, T. Balducci, V. Villicaña, A. Valencia, J. J. Gonzalez-Olvera, E. Reyes-Zamorano, and E. A. Garza-Villarreal. The mexican magnetic resonance imaging dataset of patients with cocaine use disorder: Sudmex conn. *Scientific Data*, 9(1):133, Mar 2022. 14, 16, 45

[4] K. Bachi, M. A. Parvaz, S. J. Moeller, G. Gan, A. Zilverstand, R. Z. Goldstein, and N. Alia-Klein. Reduced orbitofrontal gray matter concentration as a marker of premorbid childhood trauma in cocaine use disorder. *Frontiers in Human Neuroscience*, 12:51, 2018. 11

[5] A. Barrós-Loscertales, H. Garavan, J. C. Bustamante, N. Ventura-Campos, J. J. Llopis, V. Belloch, M. A. Parcet, and C. Ávila. Reduced striatal volume in cocaine-dependent patients. *Neuroimage*, 56(3):1021–1026, 2011. 40

[6] B. M. Caldwell, C. L. Harenski, K. A. Harenski, S. J. Fede, V. R. Steele, M. R. Koenigs, and K. A. Kiehl. Abnormal frontostriatal activity in recently abstinent cocaine users during implicit moral processing. *Frontiers in human neuroscience*, 9:565, 2015. 41

[7] V. D. Calhoun and J. Sui. Multimodal fusion of brain imaging data: a key to finding the missing link (s) in complex mental illness. *Biological psychiatry: cognitive neuroscience and neuroimaging*, 1(3):230–244, 2016. 2, 3

[8] J. Camchong, A. W. MacDonald III, B. Nelson, C. Bell, B. A. Mueller, S. Specker, and K. O. Lim. Frontal hyperconnectivity related to discounting and reversal learning in cocaine subjects. *Biological psychiatry*, 69(11):1117–1123, 2011. 9, 41

[9] R. Ciric, A. F. Rosen, G. Erus, M. Cieslak, A. Adebimpe, P. A. Cook, D. S. Bassett, C. Davatzikos, D. H. Wolf, and T. D. Satterthwaite. Mitigating head motion artifact in functional connectivity mri. *Nature protocols*, 13(12):2801–2826, 2018. 16

[10] V. Costumero, P. Rosell Negre, J. C. Bustamante, P. Fuentes-Claramonte, J. Adrián-Ventura, M.-Á. Palomar-García, A. Miró-Padilla, J. J. Llopis, J. Sepulcre, and A. Barrós-Loscertales. Distance disintegration characterizes node-level topological dysfunctions in cocaine addiction. *Addiction Biology*, 26(6):e13072, 2021. 2, 41

[11] K. E. Courtney, J. P. Schacht, K. Hutchison, D. J. Roche, and L. A. Ray. Neural substrates of cue reactivity: association with treatment outcomes and relapse. *Addiction biology*, 21(1):3–22, 2016. 41

[12] C. A. Dackis and C. P. O'Brien. Cocaine dependence: a disease of the brain's reward centers. *Journal of substance abuse treatment*, 21(3):111–117, 2001. 1

[13] L. Danon, J. Duch, A. Arenas, and A. Díaz-Guilera. Community structure identification. In *Large scale structure and dynamics of complex networks: from information technology to finance and natural science*, pages 93–114. World Scientific, 2007. 21

[14] E. Duncan, W. Boshoven, K. Harenski, E. Duncan, W. Boshoven, K. Harenski, A. Fiallos, E. Duncan, W. Boshoven, K. Harenski, et al. An fmri study of the interaction of stress and cocaine cues on cocaine craving in cocaine-dependent men. *American Journal on Addictions*, 16(3):174–182, 2007. 45

[15] K. D. Ersche, A. Barnes, P. S. Jones, S. Morein-Zamir, T. W. Robbins, and E. T. Bullmore. Abnormal structure of frontostriatal brain systems is associated with aspects of impulsivity and compulsivity in cocaine dependence. *Brain*, 134(7):2013–2024, 2011. 11

[16] O. Esteban, C. J. Markiewicz, R. W. Blair, C. A. Moodie, A. I. Isik, A. Erramuzpe, J. D. Kent, M. Goncalves, E. DuPre, M. Snyder, et al. fmriprep: a robust preprocessing pipeline for functional mri. *Nature methods*, 16(1):111–116, 2019. 16

[17] S. Gardini and A. Venneri. Reduced grey matter in the posterior insula as a structural vulnerability or diathesis to addiction. *Brain research bulletin*, 87(2-3):205–211, 2012. 11

[18] B. Garrigan, A. L. Adlam, and P. E. Langdon. The neural correlates of moral decision-making: A systematic review and meta-analysis of moral evaluations and response decision judgements. *Brain and cognition*, 108:88–97, 2016. 41

[19] E. A. Garza-Villarreal, M. M. Chakravarty, B. Hansen, S. F. Eskildsen, G. A. Devenyi, D. Castillo-Padilla, T. Balducci, E. Reyes-Zamorano, S. N. Jespersen, P. Perez-Palacios, et al. The effect of crack cocaine addiction and age on the microstructure and morphology of the human striatum

and thalamus using shape analysis and fast diffusion kurtosis imaging. *Translational psychiatry*, 7(5):e1122–e1122, 2017. 40

[20] H. Gu, B. J. Salmeron, T. J. Ross, X. Geng, W. Zhan, E. A. Stein, and Y. Yang. Mesocorticolimbic circuits are impaired in chronic cocaine users as demonstrated by resting-state functional connectivity. *Neuroimage*, 53(2):593–601, 2010. 9

[21] C. A. Hanlon, L. T. Dowdle, and J. Jones. Biomarkers for success: using neuroimaging to predict relapse and develop brain stimulation treatments for cocaine-dependent individuals. *International review of neurobiology*, 129:125–156, 2016. 2, 9

[22] C. A. Hanlon, M. J. Wesley, J. R. Stapleton, P. J. Laurienti, and L. J. Porrino. The association between frontal–striatal connectivity and sensorimotor control in cocaine users. *Drug and alcohol dependence*, 115(3):240–243, 2011. 10

[23] Y. Hu, B. J. Salmeron, H. Gu, E. A. Stein, and Y. Yang. Impaired functional connectivity within and between frontostriatal circuits and its association with compulsive drug use and trait impulsivity in cocaine addiction. *JAMA psychiatry*, 72(6):584–592, 2015. 41

[24] C. Kelly, X.-N. Zuo, K. Gotimer, C. L. Cox, L. Lynch, D. Brock, D. Imperati, H. Garavan, J. Rotrosen, F. X. Castellanos, et al. Reduced interhemispheric resting state functional connectivity in cocaine addiction. *Biological psychiatry*, 69(7):684–692, 2011. 9, 21

[25] S.-G. Kim, W. H. Jung, S. N. Kim, J. H. Jang, and J. S. Kwon. Alterations of gray and white matter networks in patients with obsessive-compulsive disorder: a multimodal fusion analysis of structural mri and dti using mcca+ jica. *PLoS One*, 10(6):e0127118, 2015. 3

[26] M. Kubicki, H. Park, C.-F. Westin, P. G. Nestor, R. V. Mulkern, S. E. Maier, M. Niznikiewicz, E. E. Connor, J. J. Levitt, M. Frumin, et al. Dti and mtr abnormalities in schizophrenia: analysis of white matter integrity. *Neuroimage*, 26(4):1109–1118, 2005. 8

[27] B. Lees, A. M. Garcia, J. Debenham, A. E. Kirkland, B. E. Bryant, L. Mewton, and L. M. Squeglia. Promising vulnerability markers of substance use and misuse: A review of human neurobehavioral studies. *Neuropharmacology*, 187:108500, 2021. 2, 41

[28] S.-J. Li, B. Biswal, Z. Li, R. Risinger, C. Rainey, J.-K. Cho, B. J. Salmeron, and E. A. Stein. Cocaine administration decreases functional connectivity in human primary visual and motor cortex as detected by functional mri. *Magnetic Resonance in Medicine: An Official Journal of the International Society for Magnetic Resonance in Medicine*, 43(1):45–51, 2000. 9

[29] X. Liang, Y. He, B. J. Salmeron, H. Gu, E. A. Stein, and Y. Yang. Interactions between the salience and default-mode networks are disrupted in cocaine addiction. *Journal of Neuroscience*, 35(21):8081–8090, 2015. 42

[30] K. O. Lim, S. J. Choi, N. Pomara, A. Wolkin, and J. P. Rotrosen. Reduced frontal white matter integrity in cocaine dependence: a controlled diffusion tensor imaging study. *Biological psychiatry*, 51(11):890–895, 2002. 8

[31] K. O. Lim, J. R. Wozniak, B. A. Mueller, D. T. Franc, S. M. Specker, C. P. Rodriguez, A. B. Silverman, and J. P. Rotrosen. Brain macrostructural and microstructural abnormalities in cocaine dependence. *Drug and alcohol dependence*, 92(1-3):164–172, 2008. 12

[32] D. M. Lipton, B. J. Gonzales, and A. Citri. Dorsal striatal circuits for habits, compulsions and addictions. *Frontiers in systems neuroscience*, 13:28, 2019. 40

[33] L. Ma, J. L. Steinberg, K. A. Cunningham, S. D. Lane, J. M. Bjork, H. Neelakantan, A. E. Price, P. A. Narayana, T. R. Kosten, A. Bechara, et al. Inhibitory behavioral control: A stochastic dynamic causal modeling study comparing cocaine dependent subjects and controls. *NeuroImage: Clinical*, 7:837–847, 2015. 10

[34] L. Ma, J. L. Steinberg, F. G. Moeller, S. E. Johns, and P. A. Narayana. Effect of cocaine dependence on brain connections: clinical implications. *Expert review of neurotherapeutics*, 15(11):1307–1319, 2015. 41

[35] L. Ma, J. L. Steinberg, Q. Wang, J. M. Schmitz, E. L. Boone, P. A. Narayana, and F. G. Moeller. A preliminary longitudinal study of white matter alteration in cocaine use disorder subjects. *Drug and alcohol dependence*, 173:39–46, 2017. 12

[36] A. T. McLellan, H. Kushner, D. Metzger, R. Peters, I. Smith, G. Grissom, H. Pettinati, and M. Argeriou. The fifth edition of the addiction severity index. *Journal of substance abuse treatment*, 9(3):199–213, 1992. 16

[37] C. S. Meade, X. Li, S. L. Towe, R. P. Bell, V. D. Calhoun, and J. Sui. Brain multimodal co-alterations related to delay discounting: a multimodal mri fusion analysis in persons with and without cocaine use disorder. *BMC neuroscience*, 22(1):1–10, 2021. 3, 13, 41

[38] V. Menon. Large-scale brain networks and psychopathology: a unifying triple network model. *Trends in cognitive sciences*, 15(10):483–506, 2011. 23, 42

[39] M. Mesulam. From sensation to cognition. brain. 121 (pt 6): 1013–1052, 1998. 41

[40] M. R. Mitchell, I. M. Balodis, E. E. DeVito, C. M. Lacadie, J. Yeston, D. Scheinost, R. T. Constable, K. M. Carroll, and M. N. Potenza. A preliminary investigation of stroop-related intrinsic connectivity in cocaine dependence: associations with treatment outcomes. *The American journal of drug and alcohol abuse*, 39(6):392–402, 2013. 10

[41] S. J. Moeller, A. B. Konova, M. A. Parvaz, D. Tomasi, R. D. Lane, C. Fort, and R. Z. Goldstein. Functional, structural, and emotional correlates of impaired insight in cocaine addiction. *JAMA psychiatry*, 71(1):61–70, 2014. 11

[42] K. P. Morie, S. W. Yip, J. Xu, K. R. Hamilton, R. Sinha, L. C. Mayes, M. N. Potenza, et al. White-matter crossing-fiber microstructure in adolescents prenatally exposed to cocaine. *Drug and alcohol dependence*, 174:23–29, 2017. 12

[43] E. J. Nestler. The neurobiology of cocaine addiction. *Science & practice perspectives*, 3(1):4, 2005. 1

[44] V. Oertel-Knöchel, B. Reinke, R. Feddern, A. Knake, C. Knöchel, D. Prvulovic, J. Pantel, and D. E. Linden. Episodic memory impairments in bipolar disorder are associated with functional and structural brain changes. *Bipolar disorders*, 16(8):830–845, 2014. 3

[45] L. Pacheco, D. Hernndez, P. Padilla, R. Velasco-Segura, J. Pacheco-Snchez, and N. Gonzalez-Garca. An fmri study on betweenness centrality in brain networks of teenagers with inhaled substance abuse disorder. *Am J Biomed Sci & Res*, 4(3):136–139, 2019. 13, 41, 42

[46] P. Paliwal, S. M. Hyman, and R. Sinha. Craving predicts time to cocaine relapse: further validation of the now and brief versions of the cocaine craving questionnaire. *Drug and alcohol dependence*, 93(3):252–259, 2008. 15

[47] V. Pando-Naude, S. Toxto, S. Fernandez-Lozano, C. E. Parsons, S. Alcauter, and E. A. Garza-Villarreal. Gray and white matter morphology in substance use disorders: a neuroimaging systematic review and meta-analysis. *Translational psychiatry*, 11(1):29, 2021. 2, 40

[48] L. Papeo, B. Agostini, and A. Lingnau. The large-scale organization of gestures and words in the middle temporal gyrus. *Journal of Neuroscience*, 39(30):5966–5974, 2019. 41

[49] J. H. Patton, M. S. Stanford, and E. S. Barratt. Factor structure of the barratt impulsiveness scale. *Journal of clinical psychology*, 51(6):768–774, 1995. 16

[50] M. Poireau, T. Milpied, A. Maillard, C. Delmaire, E. Volle, F. Bellivier, R. Icick, J. Azuar, C. Marie-Claire, V. Bloch, et al. Biomarkers of relapse in cocaine use disorder: a narrative review. *Brain Sciences*, 12(8):1013, 2022. 41

[51] J. D. Power, A. Mitra, T. O. Laumann, A. Z. Snyder, B. L. Schlaggar, and S. E. Petersen. Methods to detect, characterize, and remove motion artifact in resting state fmri. *Neuroimage*, 84:320–341, 2014. 16

[52] J. J. Prisciandaro, H. Myrick, S. Henderson, A. L. McRae-Clark, and K. T. Brady. Prospective associations between brain activation to cocaine and no-go cues and cocaine relapse. *Drug and alcohol dependence*, 131(1-2):44–49, 2013. 45

[53] J. Rasgado-Toledo, A. Shah, M. Ingalhalikar, and E. A. Garza-Villarreal. Neurite orientation dispersion and density imaging in cocaine use disorder. *Progress in Neuro-Psychopharmacology and Biological Psychiatry*, 113:110474, 2022. vi, 3, 40, 41, 45

[54] S. Ray, S. Gohel, and B. B. Biswal. Altered functional connectivity strength in abstinent chronic cocaine smokers compared to healthy controls. *Brain Connectivity*, 5(8):476–486, 2015. 9

[55] M. J. Romero, S. Asensio, C. Palau, A. Sanchez, and F. J. Romero. Cocaine addiction: diffusion tensor imaging study of the inferior frontal and anterior cingulate white matter. *Psychiatry Research: Neuroimaging*, 181(1):57–63, 2010. 12

[56] M. Rubinov and O. Sporns. Complex network measures of brain connectivity: uses and interpretations. *Neuroimage*, 52(3):1059–1069, 2010. 42

[57] J. B. Schweitzer, T. Riggins, X. Liang, C. Gallen, P. K. Kurup, T. J. Ross, M. M. Black, P. Nair, and B. J. Salmeron. Prenatal drug exposure to illicit drugs alters working memory-related brain activity and underlying network properties in adolescence. *Neurotoxicology and teratology*, 48:69–77, 2015. 13, 42

[58] D. B. Spronk, J. H. van Wel, J. G. Ramaekers, and R. J. Verkes. Characterizing the cognitive effects of cocaine: a comprehensive review. *Neuroscience & Biobehavioral Reviews*, 37(8):1838–1859, 2013. 41

[59] J. Sui, T. Adali, Q. Yu, J. Chen, and V. D. Calhoun. A review of multivariate methods for multimodal fusion of brain imaging data. *Journal of neuroscience methods*, 204(1):68–81, 2012. 2, 3, 34

[60] J. Sui, H. He, Q. Yu, J. Chen, J. Rogers, G. D. Pearlson, A. Mayer, J. Bustillo, J. Canive, and V. D. Calhoun. Combination of resting state fmri, dti, and smri data to discriminate schizophrenia by n-way mcca+ jica. *Frontiers in human neuroscience*, 7:235, 2013. 3

[61] S. F. Tapert, E. H. Cheung, G. G. Brown, L. R. Frank, M. P. Paulus, A. D. Schweinsburg, M. Meloy, and S. A. Brown. Neural response to alcohol stimuli in adolescents with alcohol use disorder. *Archives of general psychiatry*, 60(7):727–735, 2003. 41

[62] D. Tomasi, N. D. Volkow, R. Wang, J. H. Carrillo, T. Maloney, N. Alia-Klein, P. A. Woicik, F. Telang, and R. Z. Goldstein. Disrupted functional connectivity with dopaminergic midbrain in cocaine abusers. *PloS one*, 5(5):e10815, 2010. 9, 42

[63] J. Upadhyay, N. Maleki, J. Potter, I. Elman, D. Rudrauf, J. Knudsen, D. Wallin, G. Pendse, L. McDonald, M. Griffin, et al. Alterations in brain structure and functional connectivity in prescription opioid-dependent patients. *Brain*, 133(7):2098–2114, 2010. 9

[64] T. B. Üstün. *Measuring health and disability: Manual for WHO disability assessment schedule WHODAS 2.0*. World Health Organization, 2010. 16

[65] H. H. van Hell, M. Vink, L. Ossewaarde, G. Jager, R. S. Kahn, and N. F. Ramsey. Chronic effects of cannabis use on the human reward system: an fmri study. *European neuropsychopharmacology*, 20(3):153–163, 2010. 41

[66] L. Vaquero, E. Cámara, F. Sampedro, J. Perez de los Cobos, F. Batlle, J. M. Fabregas, J. A. Sales, M. Cervantes, X. Ferrer, G. Lazcano, et al. Cocaine addiction is associated with abnormal prefrontal function, increased striatal connectivity and sensitivity to monetary incentives, and decreased connectivity outside the human reward circuit. *Addiction Biology*, 22(3):844–856, 2017. 11

[67] A. Verdejo-Garcia. New insights on neurocognition in cocaine use disorder. *Current Behavioral Neuroscience Reports*, 5:232–237, 2018. 41

[68] N. D. Volkow, M. Michaelides, and R. Baler. The neuroscience of drug reward and addiction. *Physiological reviews*, 99(4):2115–2140, 2019. 1

[69] Z. Wang, J. Suh, Z. Li, Y. Li, T. Franklin, C. O'Brien, and A. R. Childress. A hyper-connected but less efficient small-world network in the substance-dependent brain. *Drug and alcohol dependence*, 152:102–108, 2015. 2, 13, 41, 42

[70] C. E. Wilcox, T. M. Teshiba, F. Merideth, J. Ling, and A. R. Mayer. Enhanced cue reactivity and fronto-striatal functional connectivity in cocaine use disorders. *Drug and alcohol dependence*, 115(1-2):137–144, 2011. 9

[71] J. Witteman, H. Post, M. Tarvainen, A. de Bruijn, E. D. S. F. Perna, J. G. Ramaekers, and R. W. Wiers. Cue reactivity and its relation to craving and relapse in alcohol dependence: a combined laboratory and field study. *Psychopharmacology*, 232:3685–3696, 2015. 41

[72] L. M. Yager, A. F. Garcia, A. M. Wunsch, and S. M. Ferguson. The ins and outs of the striatum: role in drug addiction. *Neuroscience*, 301:529–541, 2015. 40

[73] K. Yamaguchi. Drug use and its social covariates from the period of adolescence to young adulthood. some implications from longitudinal studies. *Recent Developments in Alcoholism: an Official Publication of the American Medical Society on Alcoholism, the Research Society on Alcoholism, and the National Council on Alcoholism*, 8:125–143, 1990. 34

[74] S. Zhang, W. Wang, S. Zhornitsky, and C.-s. R. Li. Resting state functional connectivity of the lateral and medial hypothalamus in cocaine dependence: an exploratory study. *Frontiers in Psychiatry*, 9:344, 2018. 41

[75] Y. Zhang, S. Zhang, J. S. Ide, S. Hu, S. Zhornitsky, W. Wang, G. Dong, X. Tang, and R. L. Chiang-shan. Dynamic network dysfunction in cocaine dependence: Graph theoretical metrics and stop signal reaction time. *NeuroImage: Clinical*, 18:793–801, 2018. 2, 41

[76] Y. Zhao, S. N. Sallie, H. Cui, N. Zeng, J. Du, T. Yuan, D. Li, D. De Ridder, and C. Zhang. Anterior cingulate cortex in addiction: new insights for neuromodulation. *Neuromodulation: Technology at the Neural Interface*, 24(2):187–196, 2021. 41